

NPS ARCHIVE
1958
AXE, J.

VORTEX FORMATIONS CAUSED BY FLUID
FLOW ACROSS A SLOT IN A FLAT PLATE

JOHN R. AXE

DUDLEY KNOX LIBRARY
NAVAL POSTGRADUATE SCHOOL
MONTEREY CA 93943-5101

VORTEX FORMATIONS CAUSED BY FLUID FLOW
ACROSS A SLOT IN A FLAT PLATE

* * * * *

John R. Axe



VORTEX FORMATIONS CAUSED BY FLUID FLOW
ACROSS A SLOT IN A FLAT PLATE

by

John R. Axe

Lieutenant, United States Navy

Submitted in partial fulfillment of
the requirements for the degree of

MASTER OF SCIENCE
IN
MECHANICAL ENGINEERING

United States Naval Postgraduate School
Monterey, California

1 9 5 8

VORTEX FORMATIONS CAUSED BY FLUID FLOW
ACROSS A SLOT IN A FLAT PLATE

by

John R. Axe

This work is accepted as fulfilling
the thesis requirements for the degree of

MASTER OF SCIENCE

IN

MECHANICAL ENGINEERING

from the

United States Naval Postgraduate School

ABSTRACT

The uniform flow of a fluid over a flat plate with a discontinuity in the form of a slot exposing a finite size cavity was investigated with the objective of determining the effect of variation of fluid velocity, slot length, and cavity size upon the frequency and stability of vortex formation. The correlating dimensionless parameters which evolve are the ratio of acoustical power to the free stream power, the acoustical quality of the resonant cavity, the Strouhal number based on the slot length, and the Reynold's number also based on the slot length.

The experimental work was performed from January 1958 through May 1958 at the United States Naval Postgraduate School, Monterey, California.

ACKNOWLEDGEMENT

The author is indebted to Professor C. P. Howard for his guidance and counsel during the complete investigation. Appreciation is also expressed to Professors P. F. Pucci, and O. B. Wilson for their advice and assistance. Grateful acknowledgement is also due Messrs R. P. Kennicott, N. Walker, K. W. Mothersell, and A. B. Rasmussen for their work in the construction, assembly and installation of the experimental equipment.

TABLE OF CONTENTS

Item	Title	Page
Chapter 1	✓ Introduction	1
Chapter 2	Description of Apparatus	3
Chapter 3	Instrumentation	9
Chapter 4	Experimental Procedure	11
Chapter 5	✓ Theory	13
Chapter 6	✓ Experimental Results	20
Chapter 7	Sources of Error	21
Chapter 8	Discussion of the Results	23
Chapter 9	Conclusions	28
Chapter 10	Recommendations	30
	Bibliography	31
Appendix I	Run Data	32
Appendix II	Plots from Data (Figures 8 through 17)	54
Appendix III	Photographs	64

TABLE OF ILLUSTRATIONS

Figure	Title	Page
1.	Velocity Profiles at a Surface of Velocity Discontinuity	1
2.	Progressive Deterioration of Surface of Velocity Discontinuity	1
3	Experimental Apparatus - Overall View	4
4	Test Section	5
5	Smoke Generator	7
6	Velocity Profile for Two Flows at Time of Union	13
7	Velocity Profile in Mixing Zone for Two Flows After Union	13
8	Frequency vs Reciprocal of Tank Height for Standing Waves	55
9	Frequency vs Reciprocal of Tank Height for Helmholtz Vibration	56
10	Velocity Profile of Flow in the Mixing Zone Without Oscillations	57
11, 12	Boundaries of Mixing Regions in the Slot	58
13	Velocity Profile of Flow in the Mixing Zone With Oscillation	59
14	Initial Boundary Layer Thickness vs Velocity	60
15	Strouhal Number vs Reynold's Number/Strouhal	61
16	Acoustical Quality and Pressure Coefficient vs Frequency	62
17	Power Ratio-Acoustical Quality vs Reynold's Number/Strouhal Number	63

Table of Symbols

A	area (ft ²)
B	a constant (in/sec)
b	half width of symmetric mixing zone (in.)
b ₀	initial boundary layer thickness (in.)
b ₁	the distance to the upper boundary of the actual mixing zone from the base line between the lip of the slot and the plate (in.)
b ₂	the distance to the lower boundary of the actual mixing zone (in.)
β	a dimensionless empirical constant = ℓ/b
C	a constant
c	the velocity of sound (ft/sec)
d	tank length = 17.0"
f	frequency (cyc/sec)
G	effective length (in.)
h	tank height, the distance measured vertically from the slot to the water level in the tank (in.)
1/h	reciprocal of h (ft ⁻¹)
j	an arbitrary constant
k	an arbitrary constant
L	slot length, the distance between the lip of the slot and the plate (in.)
ℓ	mixing length (in.)
m _{1,2,3}	mode numbers for tank
n	stage number for oscillating stream
η	a dimensionless variable = y/b
P	atmospheric pressure ("Hg)
P _a	acoustic overpressure or instantaneous pressure differential (psi)

Δp	pressure differential ("H ₂ O) average
Q	acoustical quality, dimensionless
ρ	fluid density (lbm/ft ³)
τ	shear stress in the fluid (psi)
s	jet width (in.)
T	temperature (°F)
t	time (sec)
U	free stream velocity (ft/sec)
u	instantaneous horizontal velocity of the fluid at a point (ft/sec)
u'(x)	instantaneously horizontal velocity of a particle in the central filament of a jet at x (ft/sec)
v	instantaneous vertical velocity of the fluid at a point (ft/sec)
w	slot and tank width = 8.0"
x	horizontal distance from the lip of the slot to any point (in.)
y	vertical distance from the lip of the slot to any point (in.)
ψ	a function
C _p	dimensionless pressure coefficient = $p_a / \frac{1}{2} \rho U^2$
Re	dimensionless Reynold's number = UL/ν
Str	dimensionless Strouhal number = fL/U
Z	power ratio = $C_p \text{ Str} = p_a f L / \frac{1}{2} \rho U^3$

1. Introduction

If two streams of the same fluid with different velocities unite such that their resulting flow is parallel, at the instant of union there is formed at their mutual interface a surface of velocity discontinuity (Figure 1a). Any disturbance in the surface causes an unstable distribution of the pressure, and the disturbance increases rapidly in size, while internal friction changes the surface into a fluid layer with rotation. [1]¹ The result is that the surface breaks down into eddies or vortices, usually irregular (Figure 2). [2]

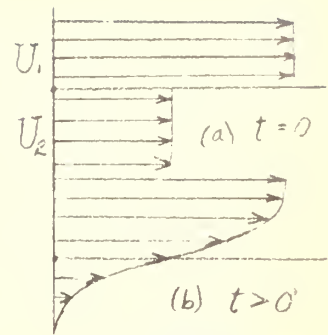


Figure 1

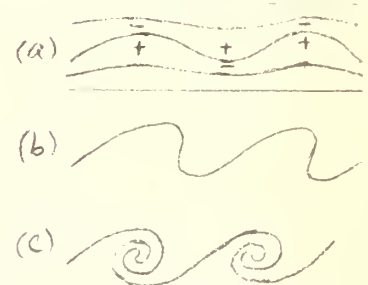


Figure 2

If a relatively thin edge is placed in the stream perpendicular to the direction of flow, under the proper circumstances, the stream will undulate and shed vortices at periodic intervals. [3]

When air is used as the fluid, this oscillatory motion produces clearly audible tones. The principle has been used for centuries in organ pipes, whistles, etc., but it wasn't until 1854 that Sondhaus [4] discovered that the resonating column was not necessary; that the tones could be produced by blowing a jet of air against an edge. Since that time "edge tones" have been a favorite subject of investigators, and though considerable work has been done, the theory is still rudimentary. Of the more important experimental studies, W. E. Benton [5] and E. G. Richardson [6] prefer an explanation based on the hydrodynamics of a

¹Numbers in brackets refer to references listed in the Bibliography.

viscous fluid, relating the phenomena to a von-Karman vortex street, where the vortices take spacings of optimum stability depending on the geometry of the system. G. B. Brown [7] takes strong exception to this hypothesis, favoring instead the theory that a compression wave travels back from the edge at acoustic velocity and triggers succeeding vortices. In a recent paper, W. L. Nyborg [8] presents a theory based on an equation of motion for the self maintained oscillations of a jet in a jet-edge system. Without attempting to justify their origin, transverse forces are assumed which act on each particle of the jet. Then the dynamical law for a particle traveling along the jet is cast in the form of a non-linear integral equation. After certain simplifying assumptions, solutions are obtained which predict the configuration of the jet with time and the frequency of oscillations.

All known previous work in this field has dealt with the effect on a thin jet flow encountering some wedge shape.

The objective of this investigation was to study the effects on a uniform flow over a flat plate which has a discontinuity in the form of a slot exposing a finite size cavity.

It was expected the effects which are produced are similar to those of jet flow, namely, the mixing of the flow and possible generation of periodic vortices.

The independent variables influencing the fluid motion which were investigated included velocity of the stream, length of slot and size of cavity.

2. Description of Apparatus

The apparatus for description purposes can be divided into six sections (Figure 3): 1) the entrance section, 2) the tunnel, 3) the test section, 4) the tank, 5) the diffuser section, and 6) the blower.

The entrance section which was covered by two 1' inch screens with $2\frac{1}{2}$ " separation, reduced the area from 34" x 25" to 8" x 10" following the countour of the Borda Mouthpiece [11] . Overall length of the entrance section was 23 $\frac{1}{4}$ ". Joints, seams, and irregularities were filled with modeling clay.

Following the entrance was the tunnel of 8" x 10" cross-section and 9 $\frac{1}{2}$ feet length.

The test section consisted of the first 13" of the tunnel over the tank (Figure 4). Sides were made of clear plastic to permit observation and photography. The bottom was a flat plate with a square edge of 0.1" thickness which was free to slide in the grooved plastic sides forming a variable slot across the tunnel over the tank. The leading edge of lip of the slot had a series of five pressure taps across the tunnel. In the top of the tunnel over the test section was a micrometer arrangement for raising and lowering various types of pressure probes, and a rubber seal permitted longitudinal traversing the first 8" of the test section.

A tank, 8" wide, 17" long, and 48" deep, was located below the test section. Provision was made for filling the tank with water to vary the volume of the air space in the tank. A glass tube, connected to both top and bottom of the tank, permitted measurement of the air space in the tank. A series of taps every 4" down one side of the tank were installed in order to probe the sound pressure distribution in the tank with a

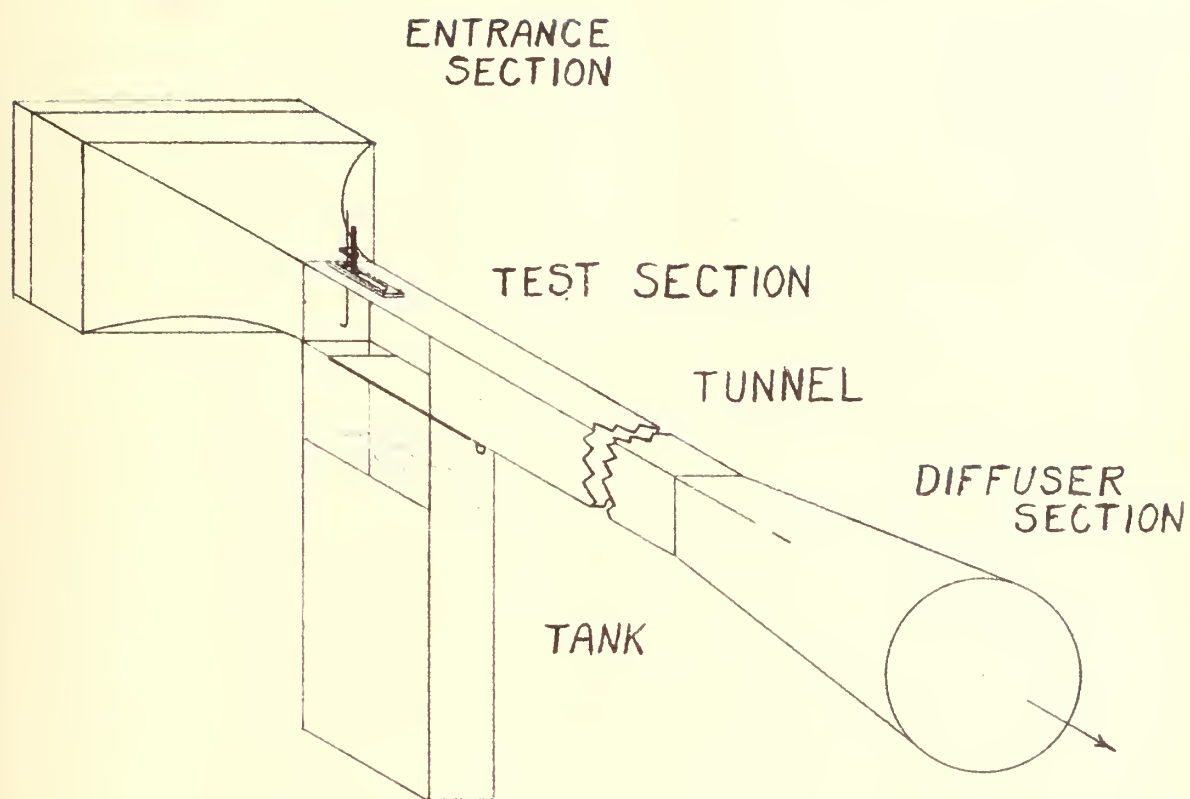
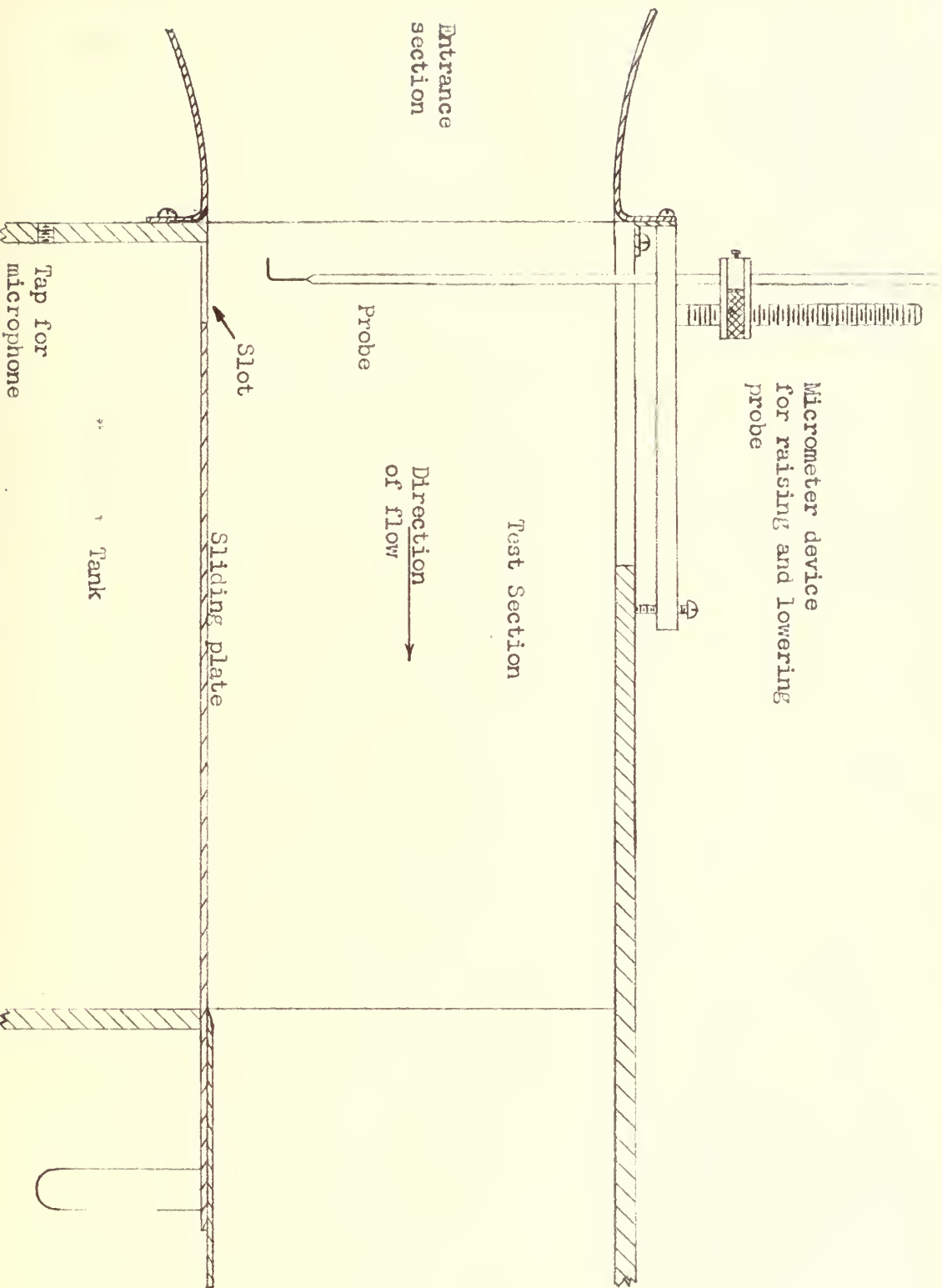


Figure 3

Experimental Apparatus - Overall View



probe microphone.

Following the tunnel was a diffuser section, which went from the 8" x 10" tunnel cross-section to a 24" circular cross-section in 40" of length. This amounted to a diffuser angle of about 23° . During early tests on the set-up, it was found that separation was occurring in the diffuser, causing surging in the tunnel velocity at the test section. To suppress the separation and eliminate the surging, vortex generators were installed in the diffuser section. These consisted of three rings made of greenfield electrical conduit. They were installed at points 3", 11", and 28" from the diffuser entrance by wiring the rings to rods placed diametrically in the diffuser. Clearance between the outer diameter of the rings and the sides of the diffuser averaged from 1" to 2". The diffuser was joined to the blower by a canvas ring.

A centrifugal blower rated at 5000 c.f.m. with 6" of water at 1800 r.p.m. was used to pull air through the tunnel. The air flow was controlled with a sliding panel choke on the blower exhaust and permitted velocities at the test section from 15.2 ft/sec to 132 ft/sec. The blower was driven by a 220 volt, 3 phase, 5 h.p. motor.

A smoke generator, for visual observation, was constructed and as finally used consisted of a combustion chamber made of a 2" steel pipe, 18" long, which sat over a settling chamber made from a large coffee can (Figure 2). The top of the combustion chamber was plugged with a cork bored to take a 3/8" pipe from a needle valve which controlled the flow of service air to the combustion chamber. A 1" garden hose, approximately 30" long, conducted the smoke from the top of the settling chamber to the entrance section of the tunnel where it was introduced in the air

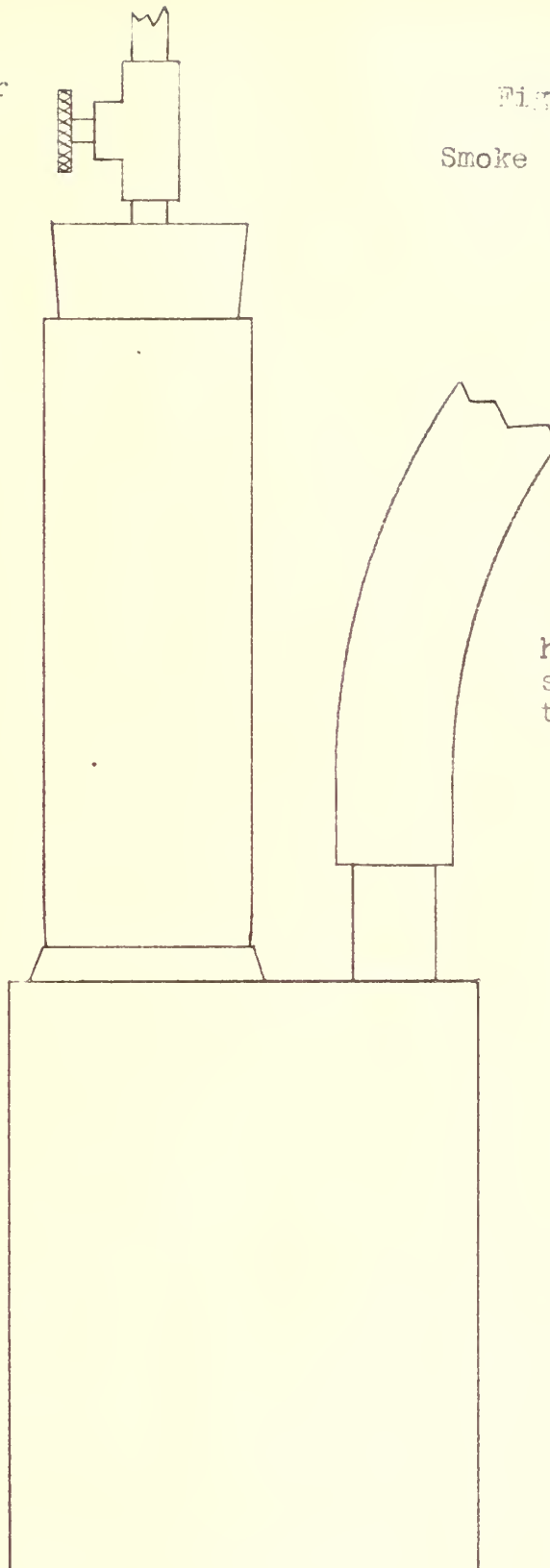
needle valve for
controlling air
supply.

Figure 5
Smoke Generator

combustion
Chamber

hose to conduct
smoke to en-
trance section

Settling
Chamber



the corners. The most satisfactory source of smoke was obtained from paper rolled tightly and wadded into the combustion chamber.

3. Instrumentation

Velocities were calculated from the pressure differential between a total head probe in the test section and the static taps immediately ahead of the slot, and were taken to be the velocity at the probe. Comparison of this method with a pitot-static probe gave substantially the same results.

Probes were largely made in the laboratory by soldering together concentric brass tubing. Barrels were made of $\frac{1}{4}$ " stock with tips of various size.

When taking velocity profiles, particularly when probing the mixing region, a micromanometer manufactured by the Flow Corp. of Cambridge, Mass. Type MM-2, was used to measure the pressure differential with graduations to .001" of water. In all other cases an ordinary oil filled manometer graduated to .01" of water up to 3" and to 0.1" above that was used.

The probe position was measured vertically with the micrometer arrangement on the top of the test section to .001" and horizontally with a graduated scale to .03".

Slot length were measured on a graduate scale to .03" and the height of water in the tank was measured similarly to 0.1".

The pickup of the generated tones was accomplished using an Altec BR 180 condenser microphone with a 3 3/16" probe, 1/16" I.D., located in the tank 4" below the slot.

The frequency was measured to one cycle with a Model 521C frequency counter and by comparison with a Model 200B audio oscillator calibrated with the counter, both manufactured by the Hewlett Packard Instrument Co. of Palo Alto, California. The amplitude of the tones were measured with a Model 400A vacuum tube volt meter and a Model 130 calibrated oscillos-

cope to .05 volts both also manufactured by the Hewlett Packard Instrument Co. Wave shapes were observed on the oscilloscope. Photographs were made with a 35mm camera and lighting was obtained from a Strobolux, Type 648A, and a Strobotac, Type 631B manufactured by the General Radio Company of Cambridge, Mass. with which visual observation could also be made.

A mercury barometer and thermometer located within 10 feet of the entrance section provided data on local atmospheric conditions.

4. Experimental Procedure

The experimental work was divided into two phases. Phase 1 was devoted to obtaining the flow characteristics of the system: velocity profiles, boundaries of the mixing region, nature of the vorticities and initial boundary layer thickness. In phase 2, the overall relationship of the various system parameters to the oscillatory motion was obtained.

Phase 1

Depending on the circumstances the type probe was selected first, and inserted in the micrometer device over the test section through the entrance section by removing the screens. After aligning the probe by eye at the lip of the slot, the screens were replaced, the blower was turned on and permitted to come up to speed. Slot length was set and velocity was adjusted to some desired value with the choke on the blower exhaust. All runs in phase 1 were conducted with the tank at maximum volume. After the micrometer device had been set to some selected position in the horizontal direction, the probe was then lowered, recording vertical probe position and pressure differential. Profiles were obtained both with and without oscillatory motion.

In addition to complete profiles, runs were conducted to determine as accurately as possible the disposition of the lower boundary in the mixing region. In these runs only the lower part of the mixing region was probed with a total head probe. When there was no oscillation of the flow a minimum pressure differential was taken as the boundary and with oscillation a zero reading on the micromanometer was taken as the boundary.

Measurements of the initial boundary layer thickness were made with a boundary layer probe at the lip of the slot. These measurements were made with the slot both opened and closed.

Photographs of flow were also taken during this phase. Due to limitations of the frequency range of the Strobolux (233 c.p.s. max.) pictures were obtainable only for the low frequency vortex formation.

Phase 2

These runs were made observing velocity, slot length, tank height, frequency, and acoustic overpressure. Various runs were made holding one or more of these system parameters constant and adjusting the remaining parameters until maximum sound pressure was obtained.

It became apparent that the tank did not amplify all frequencies equally. In order to evaluate the magnitude of the amplification, the acoustical quality of the tank as a resonator was determined over the frequency range by driving the tank with a loudspeaker located in the tunnel over the slot and measuring the sound pressure in the tank. Readings were taken at the resonant frequency and frequencies on either side of resonance at which the sound pressure was 0.707 of the resonant value for reasons to be discussed later.

5. Theory

As noted before, all known previous experimental work in this field has dealt with a jet-edge configuration. The same may be said about all known theoretical analyses except where comparison has been made to the Karman vortex street behind a cylinder. While there is no close physical resemblance between the present system and a jet-edge, the basic requirements exist. There is a union of two fluid streams of different velocity with a resulting surface of discontinuity, and a thin edge-like obstacle in the path of the mixing fluid. It was expected, therefore, that the present system was a modification of the jet-edge.

Considering first the problem of the mixing fluid which follows the breakdown of the surface of discontinuity, a solution for the velocity profile is presented by Schlichting, [9] who treats it as a problem of non-steady parallel flow.

At time t_0 , U_1 and U_2 unite at $y = 0$ (Figure 6). The situation is unstable and turbulence smoothes out the transition so that at any time after t_0 the velocity is continuous and in the mixing zone $u = u(y, t)$ and $v = 0$ (Figure 7).

Substitution of Prandtl's mixing length equation,

$$\tau = l^2 \left| \frac{\partial u}{\partial y} \right| \frac{\partial u}{\partial y}$$

1.

in the two dimensional laminar incompressible boundary layer equations,

$$\frac{\partial u}{\partial t} + u \frac{\partial u}{\partial x} + v \frac{\partial u}{\partial y} = \frac{1}{\rho} \frac{\partial \tau}{\partial y} ; \quad \frac{\partial u}{\partial x} + \frac{\partial v}{\partial y} = 0 \quad 2.$$

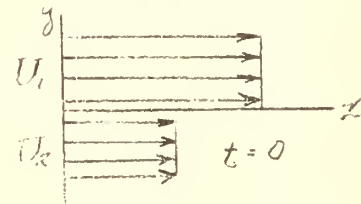


Figure 6

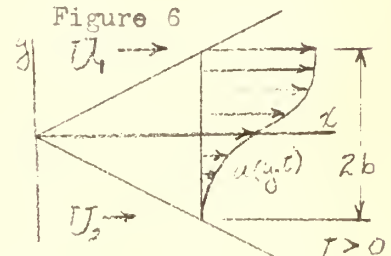


Figure 7

yields

$$\frac{\partial u}{\partial t} = \ell^2 \left| \frac{\partial u}{\partial y} \right| \frac{\partial^2 u}{\partial y^2} \quad 3.$$

Assuming similar velocity profiles, then $u = f(\eta)$, where $\eta = y/b$; a non-dimensional profile parameter and b , the half width of the mixing zone at time t after t_0 , is proportional to t . This gives

$$b = Bt; \quad \eta = y/b = y/Bt \quad 4.$$

The velocity is then assumed to be of the form

$$u = \frac{1}{2}(U_1 + U_2) + \frac{1}{2}(U_1 - U_2)\psi(\eta) \quad 5.$$

where $\psi(\eta)$ is a nondimensional stream function satisfying the continuity equation. The boundary conditions imposed are, $\psi = \pm 1$ at $\eta = \pm 1$.

Substituting these in 3., yields

$$\eta \frac{\partial \psi}{\partial \eta} + \frac{\beta C}{B} \frac{\partial \psi}{\partial \eta} \frac{\partial^2 \psi}{\partial \eta^2} = 0 \quad 6.$$

where it is assumed $\beta = \ell/b$ (an empirical constant), and $C = \frac{1}{2}(U_1 - U_2)$.

Eliminating the trivial solution $\frac{\partial \psi}{\partial \eta} = 0$, i.e., $\psi = (\text{a constant})$, which represents constant velocity, and dividing by $\frac{\partial \psi}{\partial \eta}$ leaves

$$\eta + \frac{\beta C}{B} \frac{\partial^2 \psi}{\partial \eta^2} = 0 \quad 7.$$

Integrating gives

$$\psi = C_1 \eta^3 + C_2 \eta \quad 8.$$

The boundary conditions $\psi(0) = 0$ and $\frac{\partial \psi}{\partial \eta}(\pm 1) = 0$, determine the constants $C_1 = -\frac{1}{2}$ and $C_2 = \frac{3}{2}$. The velocity profile is then

$$u(y,t) = \frac{1}{2}(U_1 + U_2) + \frac{1}{2}(U_1 - U_2) \left[\frac{3}{2} \left(\frac{y}{b} \right) - \frac{1}{2} \left(\frac{y}{b} \right)^3 \right]$$

where

$$b = \frac{3}{2} \beta^2 (U_1 - U_2) t \quad 9.$$

It may also be shown that t is proportional to x and, therefore,

$$b = (\text{a constant}) x.$$

Prandtl [2] has experimentally verified this, but in the region of no vortex formation, he has found that the same value of b , the half width, does not hold for both the upper and lower boundary of the mixing region. His results indicate that

$$b_1/x = 0.125 \text{ and } b_2/x = 0.100$$

Velocity profiles showing an inflection point of the type given by equation 9. lead to the formation of vortices. Prandtl has found experimentally that these vortices travel downstream with a velocity equal to approximately $1/2(U_1 + U_2)$. If the shedding of vortices is periodic, they will form at some frequency f , number of vortices per second, and the spacing between any two successive vortices will be $\frac{U_1 + U_2}{2f}$. If it is assumed that a new vortex forms at the lip of the slot as the center of the previous vortex reaches the plate and that each vortex travels in a straight course across the slot then

$$L = \frac{(U_1 + U_2)}{2f} \quad 10.$$

putting U_2 , the velocity in the tank, equal to zero and rearranging gives

$$\frac{fL}{U} = \frac{1}{2} \quad 11.$$

Equation 11. does not take into consideration the possibility of more than one vortex present at any time, and it is a well known fact in the jet-edge phenomena that as many as four stages are possible. [7]

Accordingly, assuming the vortices will space themselves equidistantly,

11. is modified $\frac{fL}{Un} = 1/2$

$$\text{or } \text{Str}_n = \frac{fL}{U} = \frac{n}{2} \quad 12.$$

where $n = 1, 2, 3 \dots$, is the stage number of vortex formation and corresponds to the number of vortices present at any instant, and the dimensionless ratio fL/U is defined as the Strouhal Number (Str).

For the jet-edge, by a different approach, Nyborg [8] has obtained

$$f \int_0^L dx/u'(x) = \frac{[k(k+1)]^{\frac{1}{2}}}{2} \quad 13.$$

where $k = 1, 3, 5, \dots$ which correspond to stages 1, 2, 3, ... respectively, and where $u'(x)$ corresponds to the vortex velocity.

If a constant average value of $\frac{1}{2}U$ is substituted in 13. for $u'(x)$ and the integration performed, then

$$\text{Str} = fL/U = \frac{[k(k+1)]^{\frac{1}{2}}}{4} \quad 14.$$

Also for the jet-edge, Brown [7] has obtained empirically, where $U \gg 1.3 \text{ ft/sec}$ and $L \ll 5.6''$,

$$\text{Str} = fL/U = .466j \quad 15.$$

where $j = 1, 2.3, 3.8, 5.4$ for stages 1, 2, 3, 4 respectively.

Table 1 shows the values of Str_n for the first three stages as obtained using equations 12, 14, and 15.

Table 1 - Str by various methods

eqn/ n	1	2	3
12	.500	1.000	1.500
14	.354	.866	1.370
15	.466	1.07	1.77

It was assumed above that the periodic shedding of vortices would take place. The periodic nature of the phenomena implies an element of

feedback, i.e., a given vortex influences the next succeeding vortex. [8] This influence is exerted in the form of the acoustic overpressure. In the present system the route of the feedback is through the tank which is fundamentally a resonator.

Analytical attempts to introduce the influence of the cavity were unsuccessful since the nature of the coupling and feedback mechanism is not completely understood either by the author or others [5, 6, 7, 8]. Thus a dimensional analysis approach was undertaken to determine some parameter which accounts for this phenomena. Of the parameters investigated, that of the power ratio, Z , proved to be the most useful. The power ratio is defined as $Z = \frac{p_a f L}{\frac{1}{2} \rho U^3}$ and is effectively the ratio of the power output of the cavity per unit area of the slot, to the power input from the stream per unit area of the slot. The power ratio parameter also being the product of pressure coefficient and Strouhal numbers was thus used to replace the pressure coefficient as a correlating parameter. The other non-dimensional quantities besides the Strouhal number which evolve are the Reynolds number and acoustical quality, Q . The acoustical quality being a parameter which characterizes the acoustical behavior of a resonator with its resonant frequencies.

An acoustical resonator will have two methods of vibration. First by establishing standing waves of pressure distribution with regularly spaced nodes and anti-nodes, and second by what is termed Helmholtz vibration where the entire volume of air is compressed simultaneously. [10]

In the first method, the resonant frequencies for a rectangular volume are given by a solution to the wave equation when appropriate boundary conditions are substituted.

Then from Kinsler and Frey [10]

$$f = c/2 \left[\left(\frac{m_1}{h} \right)^2 + \left(\frac{m_2}{d} \right)^2 + \left(\frac{m_3}{w} \right)^2 \right]^{-1/2} \quad 16.$$

where c is the velocity of sound, and

$$m_1 = 0, 1, 2, 3, \dots$$

$$m_2 = 0, 1, 2, 3, \dots$$

$$m_3 = 0, 1, 2, 3, \dots$$

are the mode numbers for the tank, and h , d , and w are the tank height, length, and width, respectively. The curves in figure 8 show f vs $1/h$ for various modes. The numbers in parentheses indicate (m_1, m_2) with $m_3 = 0$.

In the Helmholtz method, there is a single mode of vibration and the parameters of the system may be considered lumped. The resonant frequency is given by [10]

$$f = \frac{c}{2\pi} \sqrt{\frac{A}{GV}} \quad 17.$$

where c is the velocity of sound, A is the area of the opening in the resonator and V its volume. G is the effective length of the opening, depending on its configuration, and must be determined empirically in most cases.

An acoustical resonator is analogous to an inductance-capacitance electrical circuit. It offers a high impedance to the resonant frequency amplifying it, and a low impedance to all other frequencies, suppressing them. In both methods of vibration the acoustical quality, Q , is a measure of the acoustic impedance, and hence the amplification of the resonator. [10] Q is now defined as

$$Q = \frac{f_0}{f_1 - f_2} \quad 18.$$

where f_0 is the resonant frequency and f_1 and f_2 are the frequencies above and below resonance at which the average power is half the resonant value; and the resonant frequency for a rigid system being determined by the wave equation or Helmholtz relation. For a non-rigid system other variables such as materials, type of construction, and power of driving also influence the system, and the frequencies must be empirically determined. Since acoustical power [10] is proportional to p_a^2 then at the half power points $p_{a1} = p_{a2} = 0.707p_{a0}$.

6. Experimental Results

Experimental data are tabulated in Appendix I, and also presented in graphical form in Appendix II.

Data for phase 1 show the observed values of pressure differential, probe position in the horizontal and vertical directions, and the calculated values of velocity, velocity ratio, and position ratios.

Data from the runs for phase 2 show the observed values of frequency, slot length, tank height, pressure differential, and the voltage output of the microphone. The calculated values shown are velocity of the central stream, reciprocal of the tank height, acoustic overpressure, and the calculated dimensionless ratios: Reynold's Number, Strouhal Number, pressure coefficient, and the power ratio.

Other tabulations include the data for the calibration of the microphone, acoustical quality and resonant frequency of the tank when driven with a loudspeaker.

Included in Appendix III are a series of photographs showing the vortex formations in the slot.

7. Sources of Error

Principle sources of error in the present system lie in the inherent uncertainties in the measurements of the observed values. Based on the accuracy of the instrumentation, maximum uncertainty or uncertainty at the point of most interest for the various values is tabulated below.

Table 2 - Per cent Uncertainty

Quantity	$\pm\%$ Uncertainty
Pressure differential	4.5
Slot length	4.0
Tank height	1.0
Frequency	1.5
Voltage output of microphone	2.0
Probe position, x and y	3.0, 2.0
Velocity	2.5
Acoustic overpressure	5.0
Acoustical quality	20.0
Reynold's number	5.0
Strouhal number	5.0
Pressure coefficient	7.0
Re/Str	5.0
Power Ratio	10.0

These are the maximum uncertainties and in general improve with increasing magnitude of the quantity. Two exceptions of note are the voltage output of the microphone and the acoustical quality of the tank.

The accuracy of the vacuum tube volt meter was such that with the changing of scales approximately the same per cent uncertainty was maintained. As for the acoustical quality, the uncertainty increases with increasing magnitude, since the peaks in the resonance curve become sharper and the difference in frequency at the half power points smaller. Accordingly, the uncertainty listed above is for a high acoustical quality.

The foregoing estimate of uncertainty is based on the accuracy of the instrumentation and is in agreement with the reproducibility of results.

Other sources of error could arise from misalignment of the pressure probes, and the fact that the microphone was not located at a pressure maximum in the tank.

8. Discussion of Results

Phase 1

As seen in figure 10 the velocity profiles obtained without oscillation are similar, and in figure 11 the boundaries of the mixing zone vary linearly with x when removed from the influence of the initial boundary layer. The upper and lower slopes of the mixing zone,

$$b_1/x = 0.066 \text{ and } b_2/x = 0.191,$$

are not in agreement with the values, $b_1/x = 0.125$ and $b_2/x = 0.100$, given by Prandtl [2]. It is also obvious equation 9. does not describe the velocity profile observed in this system. This is due to the fact that equation 9. does not consider the initial boundary layer in the stream of the actual flow and also because equation 9. assumes a mixing zone symmetric with the horizontal axis.

When the stream oscillates the situation is completely changed. $v \neq 0$, the slopes of the mixing zone are no longer linear functions of x , and while velocity profiles retain the same general shape they are not similar (Figure 13), Figure 12 shows the lower boundary of the mixing zone with a construction for the assumed path a vortex would travel in traversing the slot assuming the diameter of the vortex increases linearly with x . This general pattern of travel was observed visually, and may be seen in the sequence of photographs in Appendix III, namely that the vortices do not travel straight across the slot but rather dip below the horizontal, and from figure 13 it will be seen that the average vortex velocity is more like $0.6U$ instead of $\frac{1}{2}U$ as was assumed in obtaining equations 12 and 14.

Figure 14 shows the variation of the initial boundary layer thickness



with velocity with the slot both opened and closed. In taking the data for the figure it was observed that while there was a relatively large drop in the initial boundary layer thickness when the slot was opened by even a small amount, increasing the opening did not appreciably affect it further.

The sharp increase in thickness with velocity is due to transition from a laminar to a turbulent boundary layer with the transition point passing the lip of the slot at about 25 ft/sec and moving upstream with increasing velocity.

Previous investigators of the jet-edge have all noted that there is a minimum edge distance inside which there will be no stage of oscillation. Benton [5] gives empirically as a limiting value with increasing velocity

$$L_{\min} = 1.22s$$

where s is the narrow dimension for the jet. In the present system if the initial boundary layer thickness, b_0 , is substituted for s by taking some point where the curve has flattened out, about 100 ft/sec, then

$$L_{\min} = 0.58 \text{ in.}$$

It was found in this investigation that the minimum value obtained for L for various velocities above 50 ft/sec is about 0.6 ins. No other attempts to study the influence of the boundary layer were undertaken as the entrance section was designed to keep the boundary layer small and minimize its effects.

Phase 2

Examination of figure 15 shows that the Strouhal number falls into three discreet bands with average values of 0.40, 0.95, and 1.50. These represent the stages of vortex formation for $n = 1, 2, 3$ and fall within

the range of values given in table I, page 10. As the stage number increases the stability of vortex formation and value of the pressure coefficient, C_p , decreases. Brown [7] has reported a fourth stage for jets, but higher stages were not observed in the present system.

It was indicated earlier, a very intimate coupling exists between the stream-slot and the tank, and whereas, the tank is not the source of oscillations, it does amplify them and the amplification is very selective. In fact, the net result of the above is that the stream-slot is able to oscillate only at the resonant frequency of the tank or not at all.

It has also been shown that the resonant frequency of the tank is dependent on its dimensions and its Q is highly dependent on the materials, type of construction, and the amplitude of the driving source.

In figure 8, f vs $1/h$ for the tank is compared with curves predicted by equation 16. for standing waves, and with points obtained by driving the tank with a loudspeaker and the stream-slot. It will be noted that there is a larger offset for those points obtained when driving the tank with the stream-slot. It is considered that this is caused by the change in effective volume of the tank created by the vortices.

Figure 9 shows f vs $1/h$ for the Helmholtz method of vibration. The curve shown was determined experimentally.

Figure 16 shows Q for the tank in mode (1,0) for standing waves as determined by using a loudspeaker, and C_p for stage 1 of the stream-slot at constant velocity over the same range of frequency. In addition to the large uncertainty in determining Q , it was not possible to drive the tank at the same amplitude with the loudspeaker as with the stream-slot.

The wide variation of Q suggests some other form of acoustical

contribution, possibly from the tunnel or inlet section which have resonating shapes also. However, it is evident that the correlation between Q and C_p is such that a maximum C_p will occur at points of maximum Q , when the tank vibrates in the standing wave method.

With the tank vibrating in the Helmholtz method, a maximum Q of 15 was found at 53 cyc/sec using a loudspeaker but when driving the tank with the stream-slot in stage 1 a maximum C_p of 3.11 was observed at about 65 cyc/sec for the same velocity as in figure 16. This again points out the shift in frequency caused by the vortices changing the effective volume of the tank and also indicates, despite the low Q as compared with that for standing waves, that the action of the Helmholtz method is such as to cause greater acoustic overpressures.

It has been shown that the relative magnitude of the Str determines the stage of vortex formation and that Q is the factor which correlates C_p for different frequencies in a given mode of standing wave vibration for the tank. The various variables are now combined in a single plot of $C_p Str/Q$ or Z/Q vs Re/Str (Figure 17). In figure 17 a series of runs was made in which points of maximum Q were sought at 65, 300, and 425 cyc/sec. In obtaining these points velocity and slot length were varied, and tank height was adjusted for maximum acoustic overpressure. Thus frequency was not constant but varied over a small range, accordingly it was assumed that Q remained constant where maximum acoustic overpressure was obtained, and that the shift in frequency was due to the change in effective volume of the tank.

From figure 17, it is evident that Z/Q has a maximum at about $Re/Str = 2.5 \times 10^5$ for all stages and frequencies, and that at this maximum the

value of Z/Q is the same for all stages of vortex formation for a given method of vibration of the tank. The action of the Helmholtz method in causing greater acoustic overpressures is also clearly shown where in the present system the ratio of the maximums between the Helmholtz method and the standing wave method is about 10 to 1.

9. Conclusions

1. The uniform flow of a fluid over a flat plate having a discontinuity in the form of a slot exposing a finite size cavity is held to be a modification of the jet-edge.

2. The initial boundary layer thickness determines the minimum slot length at which the stream will oscillate regardless of any other conditions, and this minimum is of the same order of magnitude as the initial boundary layer thickness.

3. Within the range of parameters investigated the Strouhal number falls into three distinct bands with average values of approximately

$$\text{Str} = 0.40 \quad \text{for Stage 1}$$

$$\text{Str} = 0.95 \quad \text{for Stage 2}$$

$$\text{Str} = 1.50 \quad \text{for Stage 3}$$

indicating the stage of oscillation of the stream, where in stage 1, one vortex is present. In stage 2, two vortices are present simultaneously, and stage 3, three vortices. Higher stages may be possible but in the present system these were not observed.

4. As the stage number increases the stability of vortex formation and the value of C_p decreases.

5. Oscillation is markedly affected by the presence of a resonator, in that a) the resonator will determine the frequency of oscillation if oscillation occurs, b) in the standing wave method the acoustic overpressure is directly proportional to the acoustical quality of the resonator, and c) when the resonator acts in the Helmholtz method its influence is such as to cause greater acoustic overpressures than the standing wave method even though Q is smaller.

6. The power ratio/acoustical quality, Z/Q , exhibits a maximum at $Re/Str = 2.5 \times 10^5$ for all stages and modes of vibration of the tank.

7. At this maximum, Z/Q is the same for all stages of vortex formation for a given method of vibration of the tank.

8. In the present system the action of the Helmholtz method of vibration in causing greater acoustic overpressures is of the order of ten times that of the standing wave method at $Re/Str = 2.5 \times 10^5$.

10. Recommendations

There is still ample room in this field for both experimental and theoretical work. In the particular phase investigated here, it is recommended in future investigations that a more accurate means of determining the acoustical quality of the resonator be found.

BIBLIOGRAPHY

1. L. Prandtl, and O. G. Tietjens, Fundamentals of Hydro- and Aeromechanics, McGraw-Hill Book Company, 1934.
2. L. Prandtl, Essentials of Fluid Dynamics, Hafner Publishing Company, 1949.
3. G. Birkhoff and E. H. Zarantonello, Jets, Wakes and Cavities, Academic Press, 1957.
4. A. Wood, Acoustics, Interscience Publishers, 1941.
5. W. E. Benton, On Edge Tones, Proceedings Physical Society, London, Vol. 38, Feb. 1926, pp. 109-126.
6. E. G. Richardson, Edge Tones, Proceedings Physical Society, London, Vol. 43, July 1931, pp. 394-404.
7. G. B. Brown, The Vortex Motion Causing Edge Tones, Physical Society, London, Vol. 49, Sept. 1937, pp. 493-507.
8. W. L. Nyborg, Jet Edge Systems, Journal of the Acoustical Society of America, Vol. 26, March 1954, pp. 174-182.
9. H. Schlichting, Boundary Layer Theory, McGraw-Hill Book Company, 1955.
10. L. F. Kinsler and A. R. Frey, Fundamentals of Acoustics, John Wiley & Sons, 1950.
11. V. L. Streeter, Fluid Dynamics, McGraw-Hill Book Company, 1948.
12. L. Prandtl and O. G. Tietjens, Applied Hydro- and Aeromechanics, McGraw-Hill Book Company, 1934.
13. Shih-I Pai, Viscous Flow Theory, Vols. 1 and 2, D. Van Nostrand Company, 1956.
14. A. H. Shapiro, The Dynamics and Thermodynamics of Compressible Fluid Flow, Vols. 1 and 2, the Ronald Press, 1954.

APPENDIX I

Run Data

APPENDIX I

RUN DATA

Phase 1

Velocity profiles without oscillation

Run 101

T = 65°F, P = 30.02"Hg

x = 0.00", L = 0.00", x/L = .000, f = 0, h = 47.5"

Total head probe 1/16" OD x 1/32" ID

y in.	y/b ₀ b = .500	Δp "H ₂ O	u '/sec	u/U
.045	.090	1.17	72.2	.785
.075	.150	1.42	79.6	.866
.100	.200	1.53	82.5	.898
.150	.300	1.71	87.3	.950
.200	.400	1.80	89.6	.975
.300	.600	1.86	91.0	.990
.400	.800	1.87	91.2	.993
.500	1.000	1.89	91.8	1.000
.750		1.89	91.8	
1.000		1.89	91.8	
1.500		1.89	91.8	
2.00		1.89	91.8	
3.00		1.90	92.0	
4.00		1.89	91.8	
5.00		1.90	92.0	
6.00		1.90	92.0	
7.00		1.90	92.0	
8.00		1.89	91.8	
9.00		1.89	91.8	

Run 102

T = 67°F, P = 29.98"Hg

x = 0.00", L = 4.20", x/L = .000, f = 0, h = 47.5"

Total head probe 1/16" OD x 1/32" ID

y in.	y/b b ₁ = .395 b ₂ = .045	Δp "H ₂ O	u '/sec	u/U
1.025		1.97	93.8	
.775		1.97	93.8	
.525		1.97	93.8	1.000

Run 102 (Continued)

y in.	y/b b ₁ = .395 b ₂ = .045	Δp "H ₂ O	u '/sec	u/U
.425	1.078	1.97	93.8	1.000
.325	.823	1.96	93.5	.996
.225	.570	1.93	92.7	.989
.175	.443	1.89	91.8	.979
.125	.316	1.82	90.0	.960
.100	.253	1.77	88.8	.946
.075	.190	1.68	86.5	.923
.050	.127	1.57	83.6	.892
.025	.063	1.35	77.8	.830
.000	.000	1.02	67.4	.719
-.010	-.222	.65	53.8	.574
-.025	-.555	.24	32.8	.350
-.050	-1.110	-.01	0.0	.000

Run 103

T = 63°F, P = 30.09"Hg

x = 1.00, L = 4.20", x/L = .238, f = 0, h = 47.5"

Total head probe 1/16" OD x 1/32" ID

y in.	y/b b ₁ = .400 b ₂ = .235	Δp "H ₂ O	u '/sec	u/U
.750		2.00	93.5	1.000
.500		2.00	93.5	1.000
.400	1.000	2.00	93.5	1.000
.300	.750	1.98	93.1	.996
.200	.500	1.94	92.1	.985
.150	.375	1.90	91.2	.975
.100	.250	1.84	89.8	.960
.050	.125	1.67	85.5	.915
.025	.063	1.49	80.8	.865
.000	.000	1.25	74.0	.791
-.025	-.106	.99	62.8	.672
-.050	-.212	.73	56.5	.605
-.075	-.318	.500	46.8	.500
-.100	-.425	.370	40.3	.431
-.125	-.531	.200	29.6	.317
-.150	-.637	.103	21.2	.227
-.175	-.744	.055	14.8	.158
-.200	-.850	.022	9.8	.102
-.225	-.955	.009	6.3	.067
-.250	-1.062	.004	4.2	.045

Run 103 (Continued)

T = 63°F, P = 30.09"Hg

x = 1.00, L = 4.20", x/L = .238, f = 0, h = 47.5"

Total head probe 1/16" OD x 1/32" ID

y in.	y/b b ₁ = .400 b ₂ = .235	Δp "H ₂ O	u '/sec	u/U
-.275		.003	3.6	.038
-.300		.002	2.9	.031
-.325		.003	3.6	.038
-.350		.004	4.2	.045

Run 104

T = 65°F, P = 30.11"Hg

x = 2.00", L = 4.20", x/L = .476, f = 0, h = 47.5"

Total head probe 1/16" OD x 1/32" ID

y in.	y/b b ₁ = .450 b ₂ = .425	Δp "H ₂ O	u '/sec	u/U
1.000		1.99	93.7	1.000
.750		1.99	93.7	1.000
.500	1.000	1.98	93.5	.997
.400	.890	1.98	93.4	.996
.300	.666	1.97	93.3	.995
.200	.445	1.93	92.4	.985
.150	.334	1.85	90.4	.965
.100	.222	1.75	88.0	.940
.050	.111	1.54	82.5	.880
.025	.056	1.34	77.0	.821
.000	.000	1.17	71.9	.767
-.050	-.118	.91	63.5	.678
-.100	-.235	.65	53.6	.572
-.150	-.353	.41	42.6	.455
-.200	-.470	.240	32.5	.347
-.250	-.588	.130	24.0	.256
-.275	-.647	.090	19.9	.212
-.300	-.705	.059	16.1	.172
-.325	-.765	.039	13.1	.140
-.350	-.824	.020	9.4	.100
-.375	-.882	.015	8.1	.086

Run 104 (Continued)

T = 65°F, P = 30.11"Hg

x = 2.00", L = 4.20" x/L = .476, f = 0, h = 47.5"

Total head probe 1/16" OD x 1/32" ID

y in.	y/b b ₁ = .450 b ₂ = .425	Δp "H ₂ O	u '/sec	u/U
-.400	- .940	.011	7.0	.075
-.425	-1.000	.008	5.9	.063
-.450		.006	5.1	.054
-.475		.005	4.7	.050
-.500		.007	5.6	.060
-.525		.007	5.6	.060

Run 105

T = 67°F, P = 30.18"Hg

x = 3.00", L = 4.20", x/L = .714, f = 0, h = 47.5"

Total head probe 1/16" OD x 1/32" ID

y in.	y/b b ₁ = .520 b ₂ = .525	Δp "H ₂ O	u '/sec	u/U
1.000		1.97	93.4	1.000
.750		1.97	93.4	1.000
.600		1.97	93.4	1.000
.500	.960	1.97	93.4	1.000
.400	.770	1.96	93.0	.996
.300	.576	1.91	91.3	.983
.200	.384	1.75	88.2	.945
.150	.288	1.63	84.8	.908
.100	.192	1.46	80.3	.860
.050	.096	1.21	73.0	.782
.000	.000	1.11	70.0	.750
-.050	-.080	.89	62.7	.672
-.100	-.130	.71	56.0	.600
-.150	-.240	.53	48.4	.518
-.200	-.320	.39	41.5	.445
-.250	-.400	.27	34.6	.371
-.300	-.480	.175	27.8	.298
-.350	-.560	.120	23.0	.246
-.400	-.640	.073	18.0	.193
-.475	-.760	.024	10.3	.110

Run 105 (Continued)

T = 67°F, P = 30.18"Hg

x = 3.00", L = 4.20", x/L = .714, f = 0, h = 47.5"

Total head probe 1/16" OD x 1/32" ID

y in.	y/b b1 = .520 b2 = .625	Δp "H ₂ O	u "/sec	u/U
-.500	-.400	.016	8.4	.090
-.525	-.840	.012	7.3	.078
-.550	-.880	.009	6.3	.067
-.575	-.920	.006	5.2	.056
-.600	-.960	.005	4.7	.050
-.650	-1.040	.006	5.2	.056
-.700		.007	5.6	.060
-.750		.009	6.3	.067

Run 106

T = 62.5°F, P = 30.32"Hg

x = 4.05", L = 4.20", x/L = .965, f = 0, h = 47.5"

Total head probe 1/16" OD x 1/32" ID

y in.	y/b b1 = .590	Δp "H ₂ O	u "/sec	u/U
.020	.034	1.13	70.0	.756
.050	.085	1.21	72.5	.784
.100	.170	1.35	76.6	.829
.150	.254	1.48	80.2	.867
.200	.339	1.60	83.5	.902
.300	.508	1.78	88.0	.951
.400	.678	1.89	90.6	.980
.450	.763	1.93	91.5	.989
.500	.848	1.94	91.9	.993
.550	.932	1.96	92.4	.998
.600	1.020	1.96	92.5	1.000
.700		1.97	92.5	1.000
1.000		1.97	92.5	1.000

Run 107

T = 67°F, P = 30.31"Hg

x = 4.25", L = 4.20", x/L = 1.01, f = 0, h = 47.5"

Total head probe 1/16" OD x 1/32" ID

y in.	y/b b ₀ =	Δp "H ₂ O	u '/sec	u/U
1.000		1.97	93.0	1.000
.750		1.97	93.0	1.000
.600		1.96	92.6	.996
.500		1.93	92.0	.989
.400		1.83	89.5	.963
.300		1.70	86.3	.928
.200		1.50	81.1	.873
.150		1.39	78.1	.840
.100		1.24	73.7	.793
.050		1.10	69.5	.747
.025		1.00	66.3	.713
.020		.93	64.0	.689

Run 108

T = 61°F, P = 30.03"Hg

x = 0.00", L = 4.20", f = 0, h = 47.5"

Total head probe 1/16" OD x 1/32" ID

y in.	y/b b ₁ = .340 b ₂ = .045	Δp "H ₂ O	u '/sec	u/U
.500		2.00	93.6	1.000
.400	1.027	2.00	93.6	1.000
.300	.769	1.97	92.9	.993
.200	.513	1.92	91.7	.980
.150	.384	1.86	90.3	.965
.100	.256	1.72	86.9	.929
.050	.128	1.49	80.9	.865
.025	.064	1.27	74.5	.795
.000	.000	.76	57.8	.618
-.015	-.333	.59	50.9	.544
-.025	-.555	.226	31.5	.337
-.030	-.667	.147	25.4	.272
-.035	-.778	.038	12.9	.138
-.040	-.889	.009	6.3	.067
-.043	-.955	.007	5.5	.059
-.045	-1.000	.000	0.0	.000
-.050		.001	2.1	.022

Lower Boundary Without Oscillation
Run 109

Total head probe 1/32" OD x 1/64" ID, $f = 0$, $h = 47.5"$

*Indicates lower boundary limit

$T = 66^{\circ}\text{F}$, $P = 30.24\text{Hg}$, $L = 4.20"$

$x = 0.50"$, $x/L = .119$, $x = 1.00"$, $x/L = .238$ $x = 1.50"$, $x/L = .357$

y in.	Δp "H ₂ O	y in.	Δp "H ₂ O	y in.	Δp "H ₂ O
-.100	.040	-.200	.013	-.250	.028
-.115	.014	-.225	.007	-.270	.020
-.120	.008	-.235*	.006	-.280	.014
-.125	.003	-.250	.006	-.290	.012
-.130*	.001			-.300	.009
-.135	.001			-.310	.007
				-.325*	.004
				-.350	.004

$x = 2.00"$, $x/L = .476$ $x = 2.50"$, $x/L = .595$ $x = 3.00"$, $x/L = .714$

y in.	Δp "H ₂ O	y in.	Δp "H ₂ O	y in.	Δp "H ₂ O
-.350	.017	-.400	.031	-.500	.025
-.370	.014	-.450	.013	-.550	.013
-.380	.011	-.465	.010	-.600	.009
-.390	.009	-.475	.008	-.625*	.008
-.400	.007	-.500*	.006	-.650	.008
-.425*	.006	-.550	.006	-.700	.008
-.450	.006				

$x = 3.50"$, $x/L = .833$

y in.	Δp "H ₂ O
-.650	.016
-.700	.014
-.725*	.012
-.750	.012

Velocity Profiles with Oscillation

Run 110

T = 67°F, P = 30.09"Hg

x = 1.00", L = 4.20", x/L = .238, f = 31.6 cyc/sec, h = 47.5"

Total head probe 1/32" OD x 1/64" ID

y in.	y/b b ₁ = .600" b ₂ = .250"	Δp "H ₂ O	u "/sec	u/U
.600	1.000	.220	31.0	1.000
.500	.833	.219	30.9	.994
.400	.667	.218	30.8	.990
.350	.583	.216	30.7	.988
.300	.500	.210	30.2	.971
.250	.427	.206	30.0	.965
.200	.192	.192	28.9	.930
.150	.250	.176	27.5	.891
.100	.167	.161	26.5	.852
.050	.083	.133	24.1	.775
.000	.000	.115	22.4	.721
-.050	-.200	.088	19.5	.625
-.100	-.400	.057	15.7	.505
-.150	-.600	.029	11.2	.360
-.175	-.700	.019	9.1	.292
-.200	-.800	.011	6.9	.222
-.225	-.900	.005	5.1	.164
-.230	-.920	.004	4.2	.135
-.240	-.960	.002	2.9	.093
-.250	-1.000	.000	0.0	.000

Run 111

T = 63°F, P = 30.17"Hg

x = 2.00", L = 4.20", x/L = .476, f = 31.6 cyc/sec, h = 47.5"

Total head probe 1/32" OD x 1/64" ID

y in.	y/b b ₁ = .600" b ₂ = .485"	Δp "H ₂ O	u "/sec	u/U
.600	1.000	.216	30.8	1.000
.500	.833	.211	30.4	.986
.400	.667	.193	29.1	.945
.300	.500	.169	27.2	.885

Run 111 (Continued)

T = 63°F, P = 30.17"Hg

x = 2.00", L = 4.20", x/L = .476, f = 31.6 cyc/sec, h = 47.5"

Total head probe 1/32" OD x 1/64" ID

y in.	y/b b ₁ = .600" b ₂ = .485"	Δp "H ₂ O	u '/sec	u/U
.200	.333	.150	25.6	.832
.100	.167	.130	23.9	.776
.000	.000	.113	22.3	.725
-.100	-.206	.092	20.1	.653
-.200	-.412	.071	17.3	.571
-.300	-.618	.049	14.7	.478
-.400	-.825	.023	10.0	.325
-.450	-.928	.011	6.3	.208
-.475	-.980	.003	2.9	.097
-.485	-1.000	.000	0.0	.000

Lower Boundary with Oscillation

Run 112

Total head probe 1/32" OD x 1/64" ID, f = 31.6 cyc/sec, h = 47.5"

x in.	b ₂ in.	x/L	b ₂ /L
.050	-.090	.119	-.021
1.00	-.250	.238	-.059
1.50	-.380	.357	-.090
1.75	-.460	.416	-.110
2.00	-.485	.476	-.116
2.25	-.490	.535	-.117
2.50	-.505	.595	-.120
2.75	-.535	.655	-.127
3.00	-.560	.714	-.133
3.50	-.650	.833	-.155

Determination of Initial Boundary

Run 113

T = 66°F, P = 30.02"Hg, Slot closed, Total head probe 1/32" OD x 1/64" ID

Δp "H ₂ O	U '/sec	b ₀ in.
.202	30.0	.290
.537	48.0	.425

Run 113 (Continued)

T = 66°F, P = 30.02"Hg, Slot closed, Total head probe 1/32" OD x 1/64" ID

Δp "H ₂ O	U '/sec	b ₀ .in
1.094	69.5	.550
2.19	96.3	.570
2.84	111.0	.580

Run 114

T = 65°F, P = 29.83"Hg, Slot open

Total head probe 1/32" OD x 1/64" ID

Δp "H ₂ O	U '/sec	b ₀ .in
.140	25.0	.100
.562	50.0	.365
1.265	75.0	.450
2.25	100.0	.475

Phase 2

Runs using a loudspeaker

Run 224 Resonant frequency determination

r(in.)	f(c/s)
40	35, 96, 179, 197, 345, 408, 440, 503, 530, 647
30	20.4, 55.7, 104, 124, 234, 247, 400, 450, 473, 608, 685
24	21.5, 27.0, 51.7, 37, 42.4, 75, 119, 137, 290, 405, 500, 555
17.2	21, 29.3, 43.5, 52, 87, 128, 154, 400, 408, 570, 820
15	33.5, 48.5, 82, 101, 119, 156, 415, 470, 612
12	34, 45, 82, 105, 146, 184, 210, 392, 408, 567, 700
10	34, 46, 67, 82, 103, 114, 181, 211, 408, 440, 699, 830

Run 225 Q determination

f_c	Δf	Q	f_c	Δf	Q
425.5	5.9	72	466.0	6.0	74
425.4	6.1	70	490.1	17.7	28
417.6	11.7	36	295.0	6.0	49
432.4	7.8	55	304.2	5.5	55
300.9	5.6	54	300.0	6.0	50
301.2	5.4	56	294.7	6.5	45
307.6	7.7	40	416.5	7.0	59
307.6	7.8	39	424.0	6.0	71
294.8	9.6	31	413.5	9.0	46
292.1	12.4	24	426.5	9.0	47
304.4	5.1	60	412.0	8.0	51
			53.0	3.5	15.2

Run 225 Calibration of Altec BR 180 Condenser Microphone

f cyc/sec	db	psi/volt	f cyc/sec	db	psi/volt
50	-77.2	.1052	330	-67.2	.0333
60	-77.0	.1027	340	-66.7	.0319
70	-76.7	.0991	350	-66.2	.0296
85	-76.3	.0947	360	-65.9	.0286
115	-75.9	.0905	370	-65.7	.0280
150	-75.1	.0826	380	-65.6	.0276
200	-73.6	.0695	390	-66.1	.0293
240	-72.1	.0585	410	-66.8	.0318
280	-70.0	.0459	430	-68.2	.0373
300	-69.0	.0409	450	-69.6	.0439
310	-68.3	.0378	470	-71.0	.0515
320	-67.8	.0357	500	-73.1	.0655

Run 201

T = 65°F P = 29.83"Hg

f cye/sec	L(in)	h(in)	$\frac{\Delta p}{H_2O}$	Volts U	ft/sec	$1/2U^2$ psi	1/h ft ⁻¹	p _a	psi	Re	$\frac{UL}{\eta}$	Str $\frac{fL}{U}$	$C_{p1} \frac{Pa}{2\rho U^2}$	Re/Str	Z
32.7	3.45	47.5	.220	25		.252				4.45 ⁴	.376		1.183 ⁵		
305	1.90	47.5	.642	50		.252				4.91	.966		5.08 ⁴		
35.4	7.05	47.5	.642	50		.252				1.825 ⁵	.417		4.37 ⁵		
303	1.22	47.5	1.345	75		.252				4.73 ⁴	.412		1.15 ⁵		
513	1.75	47.5	1.345	75		.252				6.82	.985		6.93 ⁴		
308	2.75	47.5	1.345	75		.252				1.07 ⁵	.942		1.136 ⁵		
200	4.17	47.5	1.345	75		.252				1.62	.926		1.75 ⁵		
50.5	8.30	47.5	1.345	75		.252				3.32	.465		7.28 ⁵		
35.2	9.26	47.5	1.345	75		.252				5.01	.506		9.90 ⁵		
445	1.23	47.5	2.33	100		.252				6.35 ⁴	.456		1.39 ⁵		
304	1.45	47.5	2.33	100		.252				7.50	.368		2.04 ⁵		
515	2.26	47.5	2.33	100		.252				1.17 ⁵	.970		1.207 ⁵		
445	2.45	47.5	2.33	100		.252				1.27	.930		1.366 ⁵		
308	3.93	47.5	2.33	100		.252				2.04	1.010		2.02 ⁵		
201	5.66	47.5	2.33	100		.252				2.93	.948		3.09 ⁵		
162	8.20	47.5	2.33	100		.252				4.25	1.103		3.85 ⁵		
206	9.4	47.5	2.33	100		.252				4.93	1.635		3.02 ⁵		
52	10.85	47.5	2.33	100		.252				5.65	.452		1.25 ⁶		
42	14.4	47.5	2.33	100		.252				7.47	.506		1.475 ⁶		

Run 202 T = 57°F P = 29.87"Hg

450	2.01	47.5	1.38	75		.252				8.05 ⁴	1.006		8.00 ⁴	
505	.98	47.5	2.39	100		.252				5.24	.414		1.266 ⁵	
445	1.13	47.5		100		.252				6.05	.420		1.44 ⁵	
304	1.47	47.5		100		.252				7.75	.368		2.10 ⁵	
608	1.13	47.5	4.05	133		.252				8.05	.431		1.87 ⁵	
445	1.58	47.5		133		.252				1.12 ⁵	.440		2.54 ⁵	
515	2.95	47.5				.252				2.10	.953		2.20 ⁵	
445	1.65	47.5	4.05	133		.252				1.17	.463		2.52 ⁵	
											<u>.318</u>		<u>3.68⁵</u>	
510	1.36	47.5	4.05	133		.252				1.025	.461		2.22 ⁵	

Run 203 T = 66°F P = 29.91"Hg

f cyc/sec	L(in)	h(in)	Δp H ₂ O	Volts	U ft/sec	1/2 ρU^2 psi	1/h ft ⁻¹	pa	psi	Re	$\frac{UL}{\nu}$	$\frac{Str \cdot fL}{U}$	$C_p \frac{Pa}{I/2 \rho U^2}$	Re/Str	Z
585	.95	23	4.00	132		.52				.48	.4	.350		1.85	.5
515	1.21		4.00	132		.52				8.26		.394		2.10	.5
417	1.61		4.00	132		.52				1.10	.5	.424		2.60	.5
307	1.96		4.00	132		.52				1.34		.380		3.52	.5
518	2.95		4.00	132		.52				2.02		.961		2.10	.5
420	3.55		4.00	132		.52				2.43		.945		2.57	.5
333	4.70		4.00	132		.52				3.20		.985		3.25	.5
340	7.38		4.00	132		.52				5.03		1.58		3.18	.5
174	9.33		4.00	132		.52				63.5		1.023		6.20	.5
63	12.7		4.00	132		.52				86.6		.505		1.72	.6

Run 204 T = 59°F P = 30.02"Hg

470	1.06	4.2	2.375	100	.0825	2.86				.0840	5.63	.4	.417	1.35	.5
450	1.05	5.5	2.375	100	.0825	2.22				.0009	5.57	.4	.396	1.46	.5
545	1.05	13.0	2.375	100	.0825	.92				.0199	5.57	.4	.479	1.165	.5
505	1.05	13.5	2.375	100	.0825	.83				.0316	5.57	.4	.443	1.258	.5
500	1.05	14.0	2.375	100	.0825	.857				.0324	5.57	.4	.439	1.270	.5
492	1.05	14.2	2.375	100	.0825	.845				.0324	5.57	.4	.431	1.291	.5
465	1.05	15.1	2.375	100	.0825	.795				.1356	5.57	.4	.409	1.360	.5
428	1.05	17.6	2.375	100	.0825	.682				.0785	5.57	.4	.376	1.48	.5
423	1.05	18.9	2.375	100	.0825	.635				.0242	5.57	.4	.372	1.497	.5
423	1.05	19.0	2.375	100	.0825	.632					5.57	.4	.372	1.497	.5
550													.483	1.154	.5
525	1.05	21.8	2.375	100	.0825	.550				.0254	5.57	.4	.461	1.207	.5
507	1.05	24.4	2.375	100	.0825	.492				.0434	5.57	.4	.445	1.250	.5
503	1.05	24.7	2.375	100	.0825	.485				.0382	5.57	.4	.440	1.266	.5
500	1.05	25.8	2.375	100	.0825	.465				.0088	5.57	.4	.439	1.27	.5
530	1.05	26.0	2.375	100	.0825	.461				.0046	5.57	.4	.465	1.197	.5
518	1.05	26.8	2.375	100	.0825	.484				.0179	5.57	.4	.455	1.223	.5
513	1.05	27.3	2.375	100	.0825	.440				.0374	5.57	.4	.451	1.233	.5
505	1.05	27.9	2.375	100	.0825	.430				.0379	5.57	.4	.443	1.257	.5
													.308		.142
													.526		.234
													.463		.204
													.107		.047
													.056		.026
													.216		.098
													.454		.205
													.460		.204

Run 204 (Continued)

T = 59°F P = 30.02"Hg

f	cyc/sec	L(in)	h(in)	Δp "H ₂ O	Volts	U	ft/sec	1/2 ρU^2 psi	1/h	ft ⁻¹	p _a	psi	Re $\frac{UL}{\eta}$	Str $\frac{fL}{U}$	$C_p \frac{Pa}{1/2 \rho U^2}$	Re/Str	Z
490		1.05	28.9	2.375	.451	100		.0825		.415	.0276		5.57 ⁴	.430	.335	1.294 ⁵	.144
483		1.05	30.1	2.375	.640	100		.0825		.399	.0400		5.57 ⁴	.424	.485	1.312 ⁵	.201
480		1.05	30.6	2.375	.637	100		.0825		.392	.0363		5.57 ⁴	.420	.440	1.325 ⁵	.185
475		1.05	32.3	2.375	.584	100		.0825		.372	.0318		5.57 ⁴	.417	.586	1.335 ⁵	.161
Run 205 T = 57°F P = 30.01"Hg																	
308		1.22	47.5	1.375	.490	75		.0466		.250	.0188		4.90 ⁴	.419	.404	1.17 ⁵	.1690
308		1.22	23.3	1.375	.530	75		.0466		.516	.0204		4.90 ⁴	.419	.438	1.17 ⁵	.1835
308		2.74	24.0	1.375	.530	75		.0466		.500			4.76 ⁴	.940		5.06 ⁴	
308		1.46	23.5	2.38	.530	100		.0466		.512			7.80 ⁴	.375		2.08 ⁵	
308		3.94	24.1	2.38		100				.499			2.10 ⁵	1.01		2.08 ⁵	
433		2.52	17.8	2.38		100				.675			1.30 ⁵	.910		1.43 ⁵	
328		1.51	43.0	2.38		100				.280			8.06 ⁴	.414		1.95 ⁵	
328		3.90	43.0	2.38		100				.280			2.08 ⁵	1.070		1.95 ⁵	
328		3.90	22.2	2.38		100				.542			2.08 ⁵	1.070		1.95 ⁵	
328		1.51	22.0	2.38		100				.546			8.06 ⁴	.414		1.95 ⁵	
520		.97	43.6	2.38		100				.276			5.17 ⁴	.420		1.23 ⁵	
520		.97	26.8	2.38		100				.449			5.17 ⁴	.420		1.23 ⁵	
520		.97	22.8	2.38		100				.526			5.17 ⁴	.420		1.23 ⁵	
520		.97	13.7	2.38		100				.875			5.17 ⁴	.420		1.23 ⁵	
520		.97	2.2	2.38		100				.545			5.17 ⁴	.420		1.23 ⁵	
520		2.26	13.9	2.38		100				.864			1.21 ⁵	.980		1.23 ⁵	
520		2.26	23.3	2.38		100				.515			1.21 ⁵	.980		1.23 ⁵	
520		2.26	27.1	2.38		100				.443			1.21 ⁵	.980		1.23 ⁵	
520		2.26	43.8	2.38		100				.274			1.21 ⁵	.980		1.23 ⁵	
520		1.13	43.8	4.1		132				.274			7.30 ⁴	.340		2.15 ⁵	
520		1.13	26.9	4.1		132				.445			7.30 ⁴	.340		2.15 ⁵	
520		1.13	23.0	4.1		132				.521			7.30 ⁴	.340		2.15 ⁵	

Run 205 (Continued) T = 57°F P = 30.01"Hg

f c/s	sec	L(in)	h(in)	$\frac{A}{H_2O}$	Volts	U	ft/sec	1/2 U ²	psi	Re	$\frac{UL}{\rho}$	Str $\frac{fL}{U}$	$\frac{cPa}{\rho \frac{1}{2}U^2}$	Re/Str	Z
520		1.13	13.8	4.1		132			.870	7.30\4		.340		2.15\5	
520		3.05	13.8	4.1		132			.870	2.15\5		1.00		2.15\5	
520		3.05	23.5	4.1		132			.510	2.15\5		1.00		2.15\5	
520		3.05	27.3	4.1		132			.440	2.15\5		1.00		2.15\5	
520		3.05	43.8	4.1		132			.274	2.15\5		1.00		2.15\5	
620		.91	43.8	4.1		132			.274	6.40\4		.356		1.80\5	
620		.91	15.8	4.1		132			.760	6.40\4		.356		1.80\5	
450		1.73	4.1	4.1		132			2.92	1.22\5		.493		2.48\5	
450		1.73	15.7	4.1		132			.765	1.22\5		.493		2.48\5	

Run 206 T = 58°F P = 29.78"Hg

60		.99	18.0	.11		13.2			.67	6.96\3		.376		1.85\4	
68.5		2.04	16.0	.11		13.2			.75	1.44\4		.885		1.63\4	
447		1.13	6.2	.530		45			1.93	2.72\4		.940		2.90\4	
435		1.85	17.3	.530		45			.693	4.45\4		1.49		2.98\4	
430		1.57	17.8	.420		38.6			.674	3.25\4		1.46		2.22\4	
425		1.00	17.8	.420		38.6			.674	2.06\4		.918		2.24\4	
430		1.24	17.6	.320		33.2			.681	2.20\4		1.34		1.64\4	
426		.80	17.6	.320		33.2			.681	1.42\4		.857		1.66\4	
425		.74	17.6	.950		66.2			.681	2.62\4		.397		6.60\4	
590		1.16	17.6	.950		66.2			.681	4.10\4		.862		4.75\4	
430		1.60	17.6	.950		66.2			.681	5.65\4		.866		6.52\4	
437		2.75	17.6	.950		66.2			.681	9.71\4		1.516		6.41\4	
439		3.11	17.6	1.175		69.5			.681	1.16\5		1.640		7.06\4	
440		3.46	17.6	1.50		79.2			.681	1.46\5		1.600		9.12\4	
442		4.41	17.6	2.41		101.			.681	2.38\5		1.612		1.475\5	
946		.60	17.25	4.1		133.5			.695	4.14\4		.535		7.73\4	

Run	f cye/sec	T = 65°F	P = 29.82"Hg	$\Delta_{H_2O}^p$	Volts U	ft/sec	1/2p ² psi	1/h ft ⁻¹	pa psi	Re $\frac{UL}{Re_j}$	Str $\frac{fL}{U}$	q $\frac{p_a}{1/2U^2}$	Re/Str	Z
Run 207	171	2.56	4.1	1.335	.1195	75	.0455	2.93	.00920	9.95 ⁴ / ₄	.488	.202	2.04 ⁵ / ₅	.0985
	550	2.56	13.1	1.335	.0398	75	.0455	.915	.00378	9.95 ⁴ / ₄	1.568	.083	6.35 ⁴ / ₄	.130
	342	2.56	21.2	1.335	.303	75	.0455	.565	.0094	9.95 ⁴ / ₄	.975	.207	1.02 ⁵ / ₅	.202
Run 208	543	1.34	40.0	1.085	.120	66.0	.0362	.300	.0108	4.73 ⁴ / ₄	.919	.298	5.15 ⁴ / ₄	.274
	450	1.73	40.0	1.085	.040	66.0	.0362	.300	.00176	6.10 ⁴ / ₄	.985	.0436	6.19 ⁴ / ₄	.0461
	352	2.18	40.0	1.085	.080	66.0	.0362	.300	.00234	7.70 ⁴ / ₄	.970	.0647	7.94 ⁴ / ₄	.0627
	206	3.65	40.0	1.085	.053	66.0	.0362	.300	.00360	1.29 ⁵ / ₅	.950	.0995	1.36 ⁵ / ₅	.0945
	36	9.80	40.0	1.085	.282	66.0	.0362	.300	.0296	3.46 ⁵ / ₅	.446	.819	7.75 ⁵ / ₅	.365
	468	1.50	5.3	1.085	.425	66.0	.0362	2.26	.0217	5.30 ⁴ / ₄	.890	.600	5.95 ⁴ / ₄	.335
	68	3.60	17.6	1.085	1.285	66.0	.0362	.682	.1285	1.27 ⁵ / ₅	.455	3.55	3.58 ⁵ / ₅	1.62
	430	1.62	17.6	1.085	.478	66.0	.0362	.682	.0177	5.71 ⁴ / ₄	.958	.489	1.17 ⁵ / ₅	.468
	57	5.2	25.2	1.085	.504	66.0	.0362	.476	.0525	1.84 ⁵ / ₅	.388	1.45	4.74 ⁵ / ₅	.563
	67	1.70	15.7	.224	.143	25.0	.0078	.765	.00143	6.00 ⁴ / ₄	.379	1.835	1.58 ⁵ / ₅	.0695
	33	3.75	40.5	.224	.109	25.0	.0078	.296	.00115	1.325 ⁵ / ₅	.412	.128	3.22 ⁵ / ₅	.0527
	280	2.19	26.1	4.0	2.12	133.5	.141	.460	.0975	7.73 ⁴ / ₄	.384	.690	2.02 ⁵ / ₅	.265
Run 209	55	3.0	25	.320	.138	33	.0088	.480	.0143	5.10 ⁴ / ₄	.417	1.63	1.224 ⁵ / ₅	.680
	38.8	4.5	32	.320	.090	33	.0088	.375	.00945	7.64 ⁴ / ₄	.441	1.075	1.73 ⁵ / ₅	.448
	33.5	4.5	44	.320	.141	33	.0088	.272	.0148	7.64 ⁴ / ₄	.381	1.68	2.00 ⁵ / ₅	
Run 210	520	1.50	43.7	1.055		66		.274		5.25 ⁴ / ₄	.984		5.35 ⁴ / ₄	
	68	2.90	16.4	.635		50		.731		7.58 ⁴ / ₄	.329		2.30 ⁵ / ₅	
	432	.60	16.8	.635		50		.715		1.56 ⁴ / ₄	.433		3.60 ⁴ / ₄	

Run 210 (Continued) T = 66°F P = 30.14"Hg

f cyc/sec	L(in)	h(in)	ΔP_{H_2O}	Volts	U ft/sec	$1/\rho U^2$ psi	l/h ft ⁻¹	pa psi	$Re \frac{UL}{\mu}$	Str $\frac{fL}{U}$	$\rho \frac{P_a}{17p^2}$	Re/Str	Z
470	1.92	6.0	.635		50		2.00		5.00	1.530		3.27 ⁴ / ₅	
111	2.30	6.0	.635		50		2.00		6.10	.426		1.43 ⁴ / ₅	
114	5.40	9.4	.635		50		1.28		1.41	1.030		1.37 ⁵ / ₅	
80	3.85	9.4	.635		50		1.28		1.00	.513		1.95 ⁵ / ₅	
69	3.85	13.9	.635		50		.863		1.00	.443		2.26 ⁵ / ₅	

Run 211 T = 66°F P = 30.34"Hg

461.5	.62	15.2	1.335	.60	75.6	.0454	.789	.0294	2.41	.315	.648	7.65 ⁴ / ₄	.204
427.2	.86	16.8	1.335	.86	75.6	.0454	.714	.0318	3.35	.406	.700	8.25 ⁴ / ₄	.284
354	1.10	19.8	1.335	.41	75.6	.0454	.605	.0119	4.28	.425	.262	1.008 ⁵ / ₅	.1115
335	1.14	20.9	1.335	.73	75.6	.0454	.574	.0236	4.44	.420	.520	1.06 ⁵ / ₅	.218
320	1.18	22.1	1.335	.54	75.6	.0454	.543	.0192	4.59	.415	.423	1.11 ⁵ / ₅	.175
301	1.24	23.6	1.335	.77	75.6	.0454	.508	.0304	4.83	.410	.670	1.18 ⁵ / ₅	.275
271	1.37	26.6	1.335	.43	75.6	.0454	.451	.0211	5.33	.409	.465	1.305 ⁵ / ₅	.190
226	1.74	32.3	1.335	.28	75.6	.0454	.371	.0174	6.77	.433	.384	1.57 ⁵ / ₅	.166
445	.80	15.8	1.335	.31	75.6	.0454	.759	.0132	3.12	.392	.291	7.95 ⁴ / ₄	.114
416	.90	18.2	1.335	.39	75.6	.0454	.659	.0131	3.50	.412	.289	8.49 ⁴ / ₄	.119

Run 212 T = 65°F P = 30.33"Hg

451	.70	15.25	1.385	.51	75.6	.0471	.786	.0240	2.74	.353	.510	7.75 ⁴ / ₄	.1800
446	.80	15.8	1.385	.35	75.6	.0471	.758	.0151	3.14	.394	.321	7.96 ⁴ / ₄	.1265
436	.84	16.2	1.385	.55	75.6	.0471	.740	.0215	3.29	.404	.456	8.14 ⁴ / ₄	.184
424	.88	16.9	1.385	.72	75.6	.0471	.710	.0260	3.45	.411	.552	8.38 ⁴ / ₄	.227
354	1.10	19.8	1.385	.35	75.6	.0471	.605	.0133	4.31	.429	.282	1.005 ⁵ / ₅	.121
335	1.14	20.9	1.385	.65	75.6	.0471	.574	.0211	4.47	.421	.448	1.061 ⁵ / ₅	.188

Run 213 T = 68°F P = 29.92"Hg

f c/c/sec	L(in)	h(in)	ΔP_{H_2O}	Volts	U ft/sec	$1/2 \rho U^2$ psi	l/h ft-l	p_a psi	$Re_{\frac{UL}{\mu}}$	$\frac{UL}{\tau}$	Str	$\frac{fL}{U}$	$C_p \frac{p_a}{1/2 \rho U^2}$	Re/Str	Z
65.3	1.40	14.5	.165	.072	20.5	.00343	.826	.0072	1.48	\backslash^4	.371	2.10	3.98	\backslash^4	.779
65.3	1.52	14.7	.185	.090	22.6	.00415	.815	.0090	1.77		.366	2.17	4.85		.794
65.7	1.66	15.4	.240	.165	27.5	.00615	.778	.0165	2.34		.330	2.68	7.09		.884
66.2	2.04	15.9	.310	.212	32.7	.00867	.754	.0212	3.41		.344	2.44	9.90	\backslash^5	.839
66.2	2.35	16.1	.425	.413	39.8	.0123	.745	.0413	4.78		.326	3.23	1.467	\backslash^5	1.053
66.7	2.74	16.5	.500	.610	46.7	.0155	.726	.0610	6.53		.326	3.94	2.00		1.286
66.2	3.02	16.9	.685	.729	52.4	.0222	.709	.0729	8.09		.318	3.28	2.54		1.044
67.2	3.27	16.8	.825	.900	57.6	.0273	.713	.0900	9.65		.318	3.30	3.04		1.050
66.7	3.57	17.5	1.00	1.220	64.4	.0336	.685	.1220	1.084	\backslash^5	.308	3.63	3.52		1.120
67.2	3.89	17.5	1.145	1.406	69.2	.10388	.685	.1406	1.375		.315	3.62	4.36		1.140
66.7	4.27	18.1	1.25	1.325	72.5	.0426	.662	.1325	1.584		.328	3.11	4.83		1.020
67.2	5.14	18.5	1.705	1.700	84.8	.0591	.648	.1700	2.33		.340	2.87	6.85		.975
67.2	5.23	19.6	1.85	1.857	88.5	.0644	.614	.1857	2.47		.331	2.88	7.45		.954
68.1	7.62	19.5	2.69	1.935	107.3	.0946	.617	.1935	4.37		.403	2.04	1.084	\backslash^6	.821

Run 214 T = 58°F P = 29.77"Hg

295	.94	23.7	.675	.093	51.6	.0218	.506	.00386	2.59	\backslash^4	.447	.177	5.79	\backslash^4	.079
296	1.07	23.7	.890	.223	60.1	.0296	.506	.00925	3.44		.438	.312	7.85		.137
297	1.13	23.7	1.17	.425	69.5	.0397	.506	.0765	4.19		.401	.444	1.043	\backslash^5	.178
296	1.18	23.7	1.375	.650	75.7	.0471	.506	.0270	4.77		.384	.573	1.243		.220
296	1.27	23.8	1.745	1.050	85.9	.0605	.504	.0436	5.82		.365	.720	1.595		.263
296	1.40	23.9	2.25	1.490	98.0	.0788	.502	.0619	7.33		.352	.785	2.08		.276
296	1.53	24.0	2.67	1.835	107.0	.0940	.500	.0762	8.74	\backslash^5	.352	.810	2.48		.285
295	1.67	24.1	3.1	2.18	115.0	.110	.498	.0905	1.028		.356	.824	2.88		.293
295	1.91	24.2	4.0	2.50	131.0	.142	.496	.1038	1.335		.358	.730	3.72		.262

Run	215	T = 60°F	P = 30.01"Hg											
	f cyc/sec	L(in)	h(in)	ΔP_{H_2O}	Volts	U ft/sec	$1/2 \rho U^2$ psi	1/h ft ⁻¹	p _a psi	$Re_{\frac{UL}{\mu}}$	$\frac{Str \cdot L}{U}$	$C_{pL} \frac{Pa}{Pl/2 \mu^{1/2}}$	Re/Str	Z
299	1.05	23.53	.945	.160	61.8	.0313	.510	.0065	3.42 ⁴	.423	.208	8.07 ⁴	.088	
300	1.22	23.53	1.355	.63	74.8	.0461	.510	.0256	4.80	.408	.555	1.176 ⁵	.227	
300	1.30	23.53	1.82	1.13	87.5	.0655	.510	.0460	5.99	.371	.702	1.615	.261	
299	1.44	23.68	2.51	1.77	100.4	.0827	.506	.0720	7.63 ⁴	.357	.870	2.14 ⁵	.311	
300	1.60	23.60	2.945	2.24	112.0	.1034	.508	.0911	9.45	.357	.883	2.65	.316	
300	2.01	23.68	4.05	2.80	132.0	.1435	.506	.1140	1.40 ⁵	.380	.795	3.68	.302	
Run	216	T = 51°F	P = 29.85"Hg											
428	.75	16.7	1.06	.478	65.9	.0358	.719	.0177	2.66 ⁴	.407	.494	6.53 ⁴	.201	
423	.86	17.0	1.37	.810	75.5	.0470	.705	.0288	3.49	.402	.612	8.67	.246	
421	.94	17.2	1.76	1.515	86.0	.0610	.697	.0530	4.35	.384	.869	1.132 ⁵	.334	
419	1.02	17.4	2.21	2.44	96.8	.0774	.690	.0841	5.30	.368	1.089	1.44	.400	
418	1.10	17.5	2.82	4.04	109.9	.0905	.685	.1384	6.50	.348	1.390	1.87	.484	
418	1.22	17.5	3.45	5.31	121.0	.126	.685	.182	7.93	.351	1.444	2.26	.506	
419	1.27	17.5	4.05	6.37	131.6	.144	.685	.220	8.97	.337	1.53	2.66	.515	
Run	217	T = 60°F	P = 30.01"Hg											
425	.75	16.50	.945	.150	61.8	.0313	.726	.0054	2.44 ⁴	.430	.1725	5.67 ⁴	.074	
425	.84	16.68	1.445	.750	77.5	.0495	.719	.0270	3.43	.384	.543	8.92	.209	
426	.92	16.60	1.95	1.70	90.6	.0675	.722	.0611	4.40	.360	.906	1.22 ⁵	.326	
424	.99	16.75	2.43	3.00	101.6	.0849	.715	.1080	5.30	.344	1.274	1.54	.438	
425	1.05	16.80	2.905	4.00	111.4	.1020	.714	.144	6.16	.334	1.413	1.845	.472	
426.5	1.24	16.76	4.05	5.80	132.0	.143	.715	.209	8.63	.334	1.460	2.58	.488	
Run	218	T = 61°F	P = 29.85"Hg											
67.2	3.80	20.1	.19	.045	23.0	.00398	.596	.0045	4.59 ⁴	.925	1.13	4.95 ⁴	1.046	
68.7	4.90	19.6	.29	.074	31.2	.00795	.612	.0074	8.02	.900	.93	8.90	.837	
69.2	5.70	20.4	.375	.087	36.7	.0110	.588	.0087	1.097 ⁵	.896	.79	1.224 ⁵	.709	
70.6	6.75	21.3	.49	.111	43.1	.0152	.563	.0111	1.53	.922	.78	1.66	.674	
70.2	8.05	19.0	.605	.212	48.6	.0193	.631	.0212	2.05	.969	1.10	2.12	1.066	
69.2	9.00	21.0	.73	.318	54.0	.0252	.571	.0318	2.55	.961	1.26	2.65	1.212	

Run	f cpy/sec	T = 58°F	L(in)	h(in)	ΔP_{H_2O}	Volts	U ft/sec	$1/2 \rho U^2$ psi	$1/h$ ft ⁻¹	pa psi	$Re_{\frac{UL}{\nu}}$	$Str \frac{fL}{U}$	$C_{fL/2\rho U^2}$	Re/Str	Z
Run 219		P = 29.77"Hg													
299		1.34	23.9		.395	.0848	37.8	.0118	.503	.00347	2.70 ^{1/4}	.885	.294	3.05 ^{1/4}	.260
299		1.70	23.8		.555	.1431	46.2	.0175	.505	.00585	4.20 ^{1/4}	.916	.335	4.58	.307
300		2.14	24.0		.82	.191	57.5	.0271	.500	.00781	6.41 ^{1/4}	.930	.288	6.90 ^{1/4}	.268
300		2.53	24.2		1.175	.276	69.7	.0400	.496	.0113	9.41 ^{1/5}	.906	.282	1.04 ^{1/5}	.256
302		2.79	24.1		1.435	.382	77.5	.0494	.498	.0156	1.15 ^{1/5}	.905	.316	1.275	.286
302		3.19	24.2		1.855	.544	88.6	.0645	.496	.0222	1.51	.896	.344	1.685	.308
302		3.71	24.3		2.36	.690	100.4	.0829	.494	.0262	1.99	.929	.340	2.14	.316
302		4.13	24.6		3.15	.850	116.0	.111	.488	.0347	2.56	.896	.311	2.85	.279
301		4.85	25.2		4.1	.995	132.5	.146	.476	.0406	3.43	.918	.278	3.74	.255
Run 220		T = 60°F			P = 30.01"Hg										
299		1.88	23.86		.645	.125	50.0	.0205	.503	.0051	4.95 ^{1/4}	.936	.247	5.29 ^{1/4}	.231
301		2.34	23.87		.940	.190	61.5	.0312	.503	.0077	7.59	.954	.247	7.95	.236
300.5		2.84	24.03		1.350	.310	74.7	.0460	.500	.0126	1.12 ^{1/5}	.952	.274	1.175 ^{1/5}	.261
301		3.21	24.25		1.845	.570	88.0	.0638	.495	.0231	1.49	.915	.363	1.63	.332
301.5		3.70	24.37		2.480	.790	102.6	.0866	.493	.0320	2.00	.905	.370	2.21	.335
302		4.46	24.48		3.30	.980	119.0	.1160	.490	.0397	2.80	.944	.342	2.96	.323
Run 221		T = 57°F			P = 29.85"Hg										
420		1.24	17.2		.59	.228	47.7	.0188	.698	.0081	3.18 ^{1/4}	.909	.431	3.50 ^{1/4}	.392
423		1.35	17.2		.705	.276	52.8	.0230	.698	.0098	3.83	.901	.426	4.25	.384
421		1.45	17.5		.81	.329	57.0	.0268	.685	.0117	4.44	.891	.436	4.98	.389
422		1.70	17.6		1.09	.504	66.9	.0368	.682	.0179	6.10	.895	.486	6.81	.435
423		1.96	17.6		1.39	.650	76.0	.0477	.682	.0231	8.00	.910	.484	8.80	.440
424		2.20	17.8		1.735	.862	85.5	.0601	.675	.0306	1.01 ^{1/5}	.910	.508	1.111 ^{1/5}	.462
421		2.52	18.4		2.185	1.160	96.4	.0765	.652	.0415	1.303	.917	.542	1.42	.497
425		2.85	17.8		2.81	1.593	109.7	.0990	.675	.0566	1.680	.920	.572	1.825	.526
423		3.18	18.2		3.4	1.99	120.0	.120	.660	.0707	2.05	.934	.589	2.20	.540
424		3.49	18.5		4.1	2.34	132.4	.146	.649	.0831	2.48	.930	.570	2.67	.530

Run 222 T = 570F P = 30.15"Hg

f cyc/sec	L(in)	h(in)	ΔP H ₂ O	Volts	U ft/sec	$1/2 \rho U^2$ psi	l/h ft ⁻¹	p _a psi	$\frac{UL}{Re^2}$	$\frac{Str \cdot L}{U}$	$C \frac{P_a}{Pl^2 \rho U^2}$	Re/Str Z
300	4.09	24.9	1.08	.0398	66.0	.0363	.482	.00161	$1.44 \sqrt[5]{5}$	1.550	.0443	$9.28 \sqrt[4]{4}$.0686
300	4.44	24.9	1.255	.0690	71.5	.0429	.482	.00279	1.696	1.552	.0650	$1.09 \sqrt[5]{5}$.1010
302	5.00	25.3	1.66	.154	83.0	.0573	.475	.00622	2.22	1.508	.1085	$1.472 \sqrt[5]{5}$.1638
301	5.56	25.6	2.04	.228	92.2	.0710	.469	.00920	2.74	1.510	.1297	1.815 .1960
302	6.14	25.9	2.435	.289	101.1	.0854	.464	.01168	3.32	1.525	.1367	2.18 .208

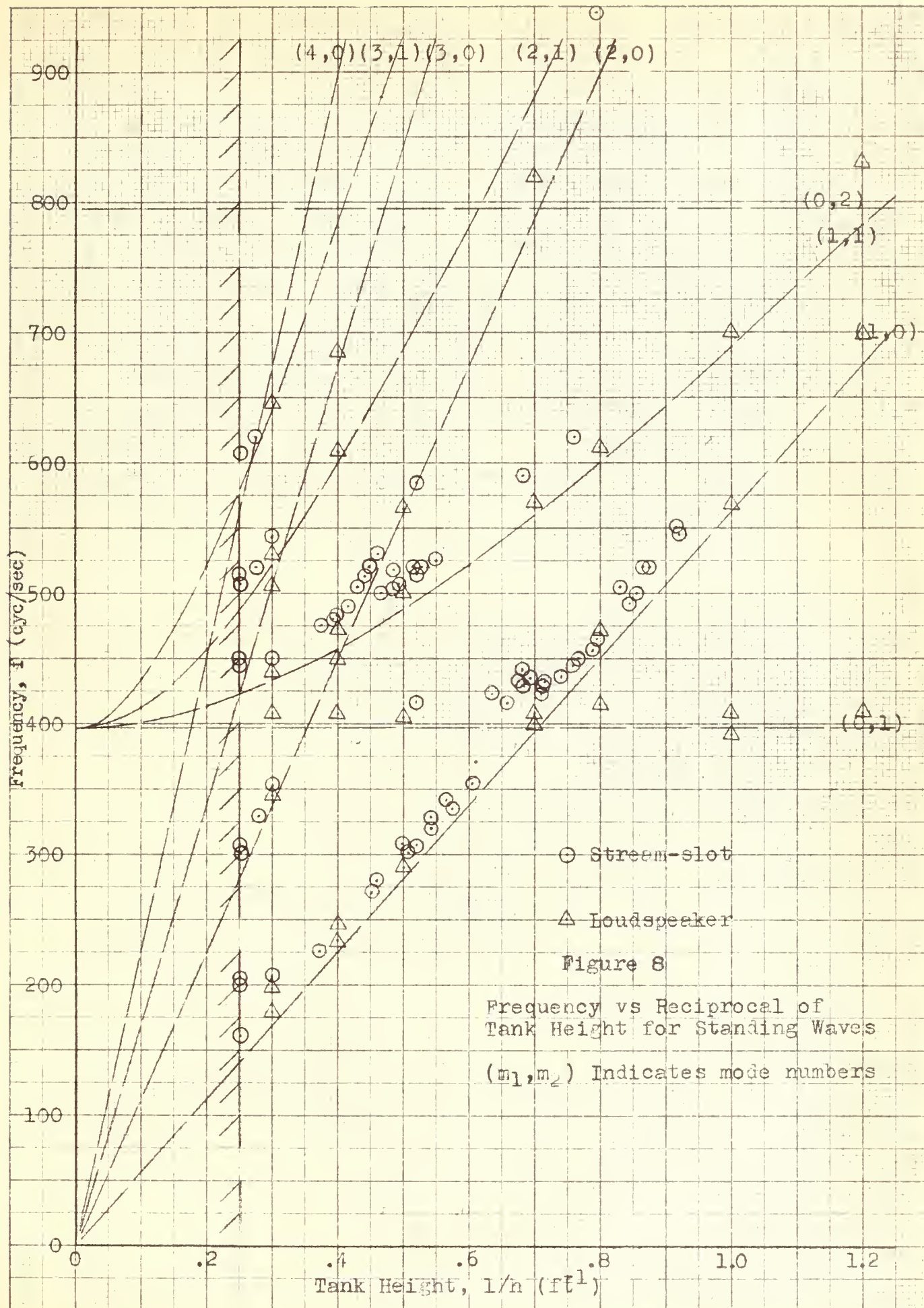
Run 223 T = 570F P = 30.15"Hg

424	1.46	17.3	.385	.0398	36.7	.0112	.694	.00143	$2.86 \sqrt[4]{4}$	1.405	.128	$2.04 \sqrt[4]{4}$.180
421	1.86	17.5	.520	.0636	43.9	.0161	.685	.00229	4.35	1.490	.142	2.92 .212
426	2.18	17.5	.670	.0716	50.9	.0215	.685	.00258	5.91	1.520	.120	3.89 .1825
426	2.72	17.7	.955	.0663	61.8	.0318	.678	.00239	8.97	1.562	.0752	5.75 .1175
426	3.36	18.0	1.365	.0557	74.8	.0466	.666	.00201	$1.34 \sqrt[5]{5}$	1.597	.0430	8.39 .0686
424	3.84	18.4	1.795	.1355	86.4	.0621	.652	.00488	1.78	1.572	.0785	$1.13 \sqrt[5]{5}$.1235
424	4.45	18.6	2.42	.1805	101.0	.0847	.645	.00650	2.40	1.590	.0767	1.51 .1220

APPENDIX II

Plots From Data

Figures 8 through 17



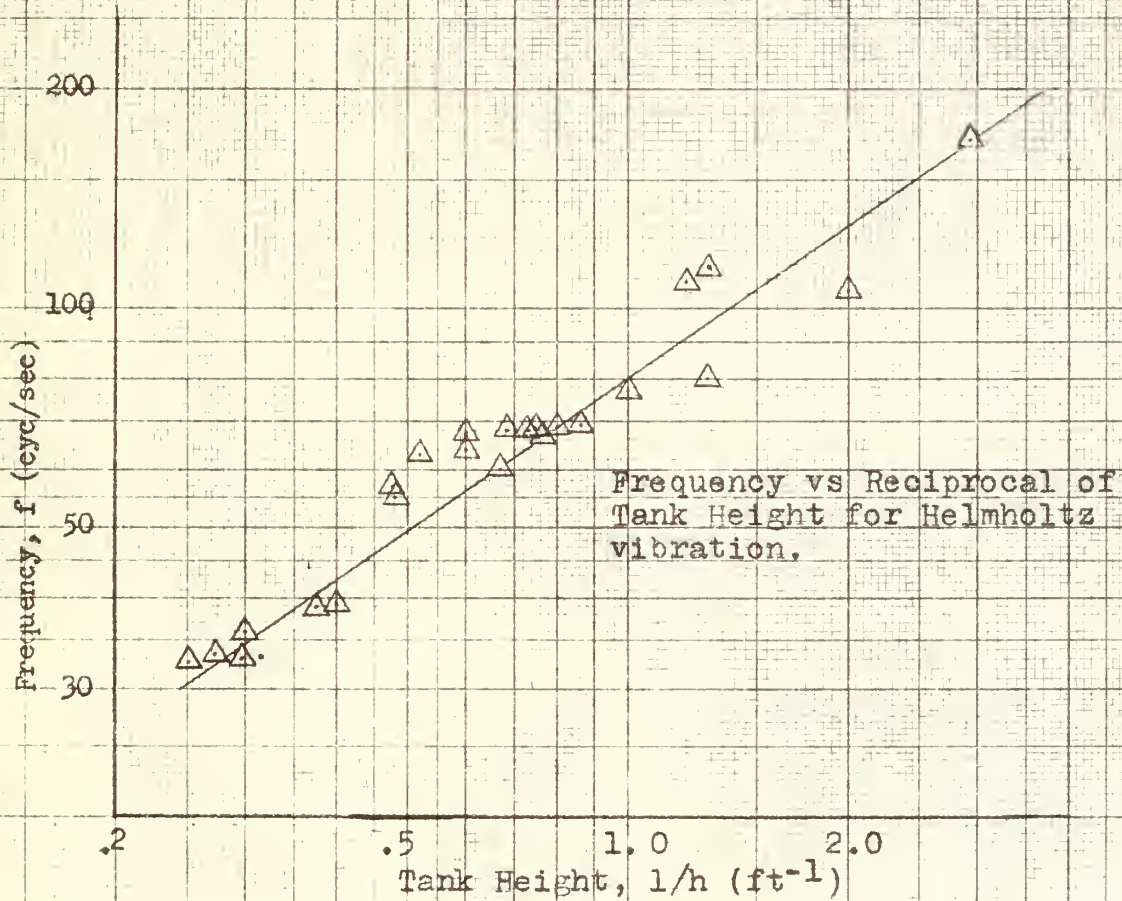


Figure 9

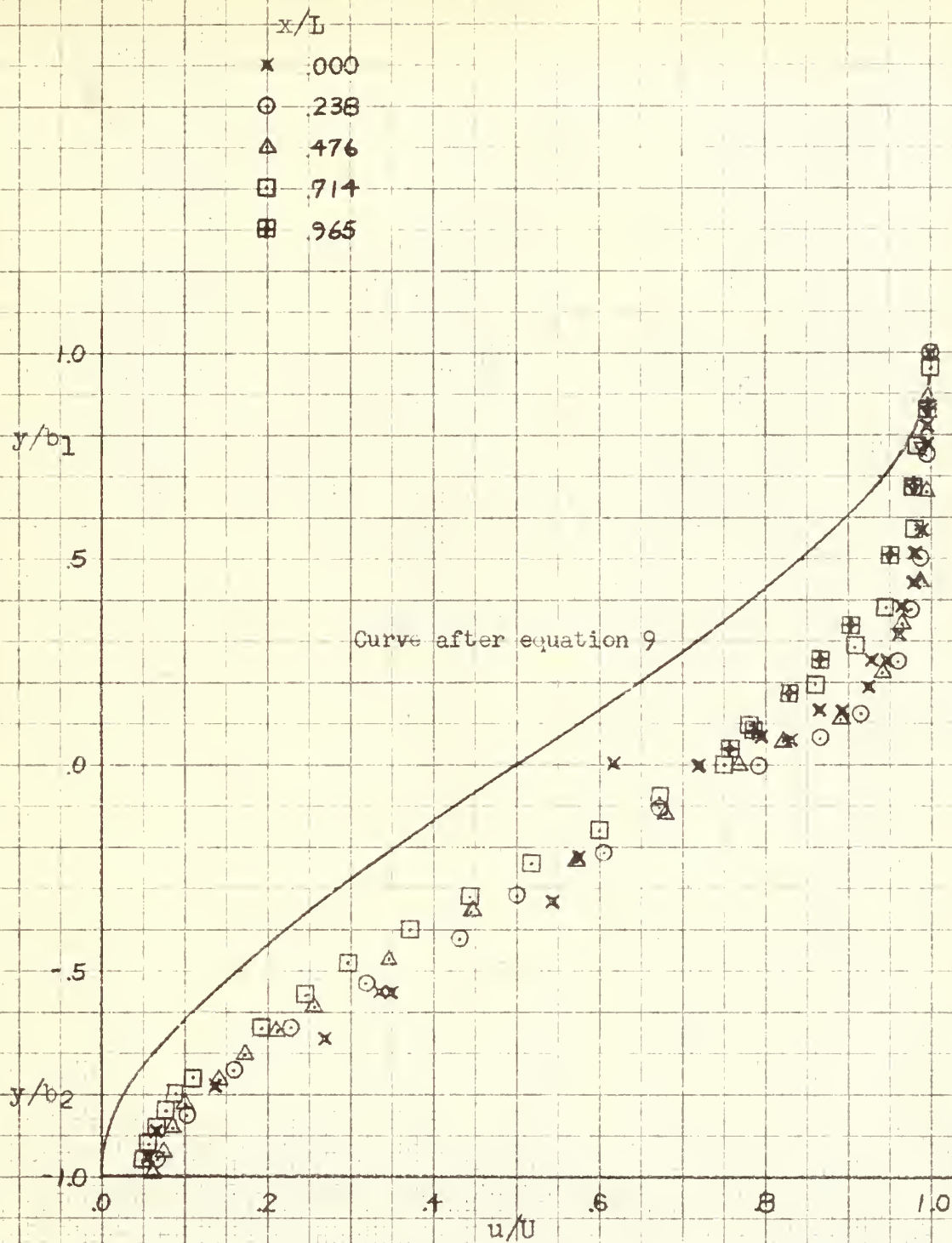
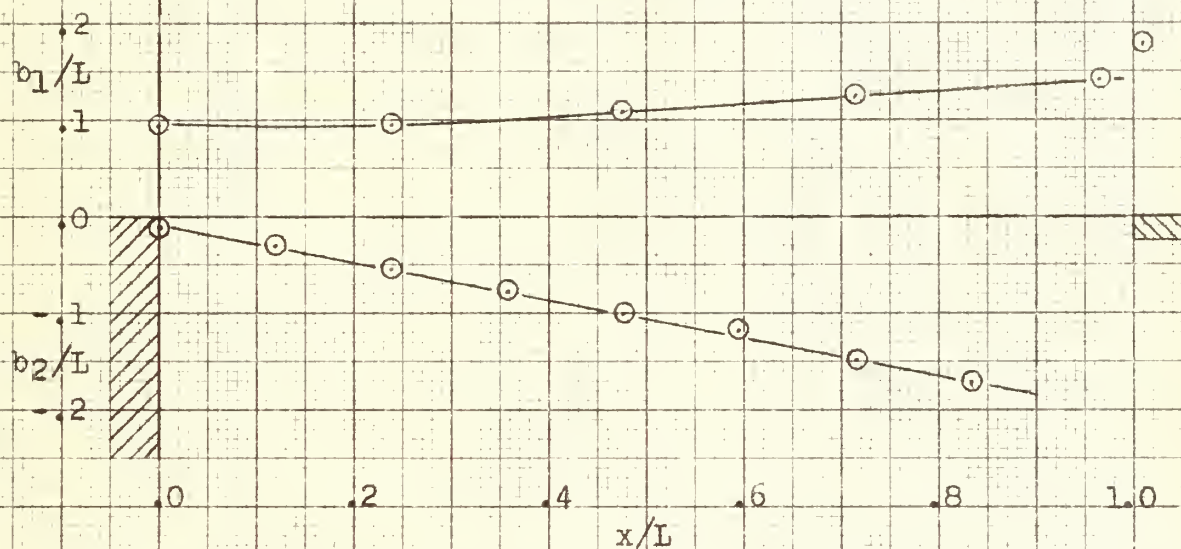


Figure 10

Velocity profile of flow in the mixing zone without oscillations.

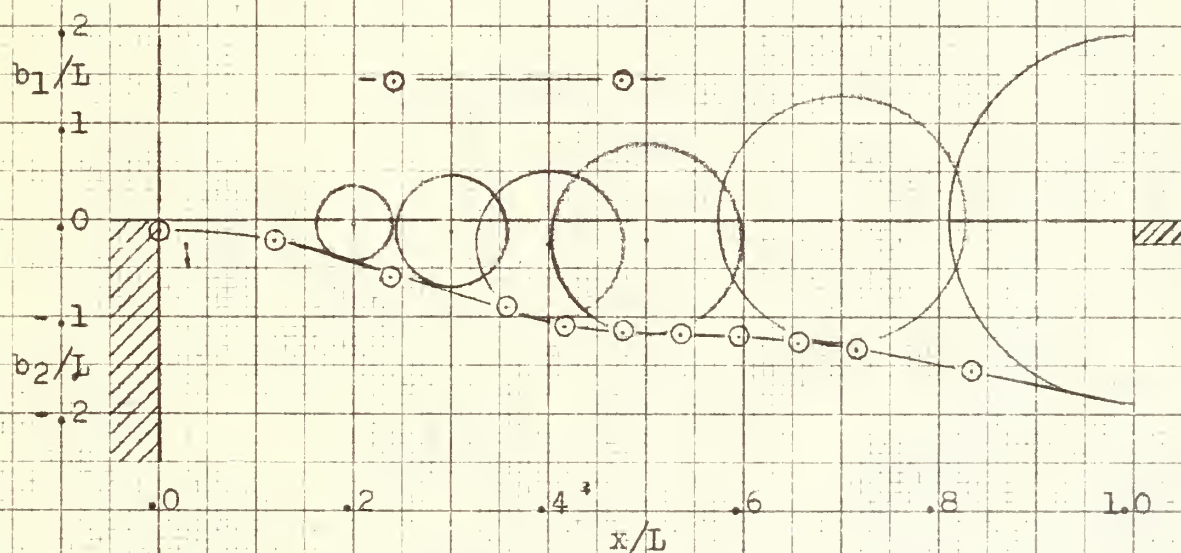
Boundaries of mixing regions in the slot

Figure 11



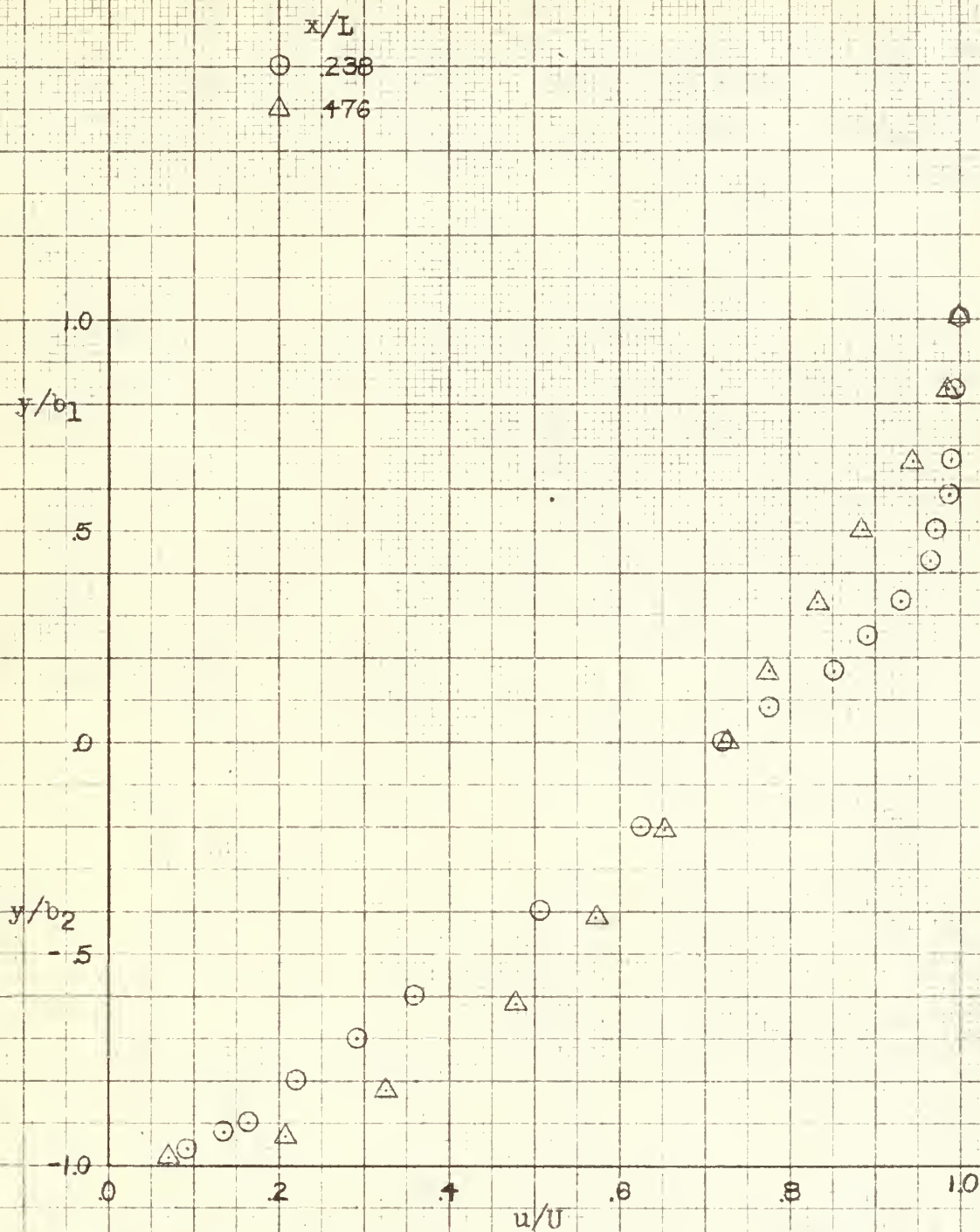
Without oscillation.

Figure 12



With oscillation, $f = 32$ cyc/sec.

Construction shows successive positions of a vortex traveling across the slot, assuming rate of growth to be constant with x .



Velocity profile of flow in the mixing zone with oscillation.

Figure 13

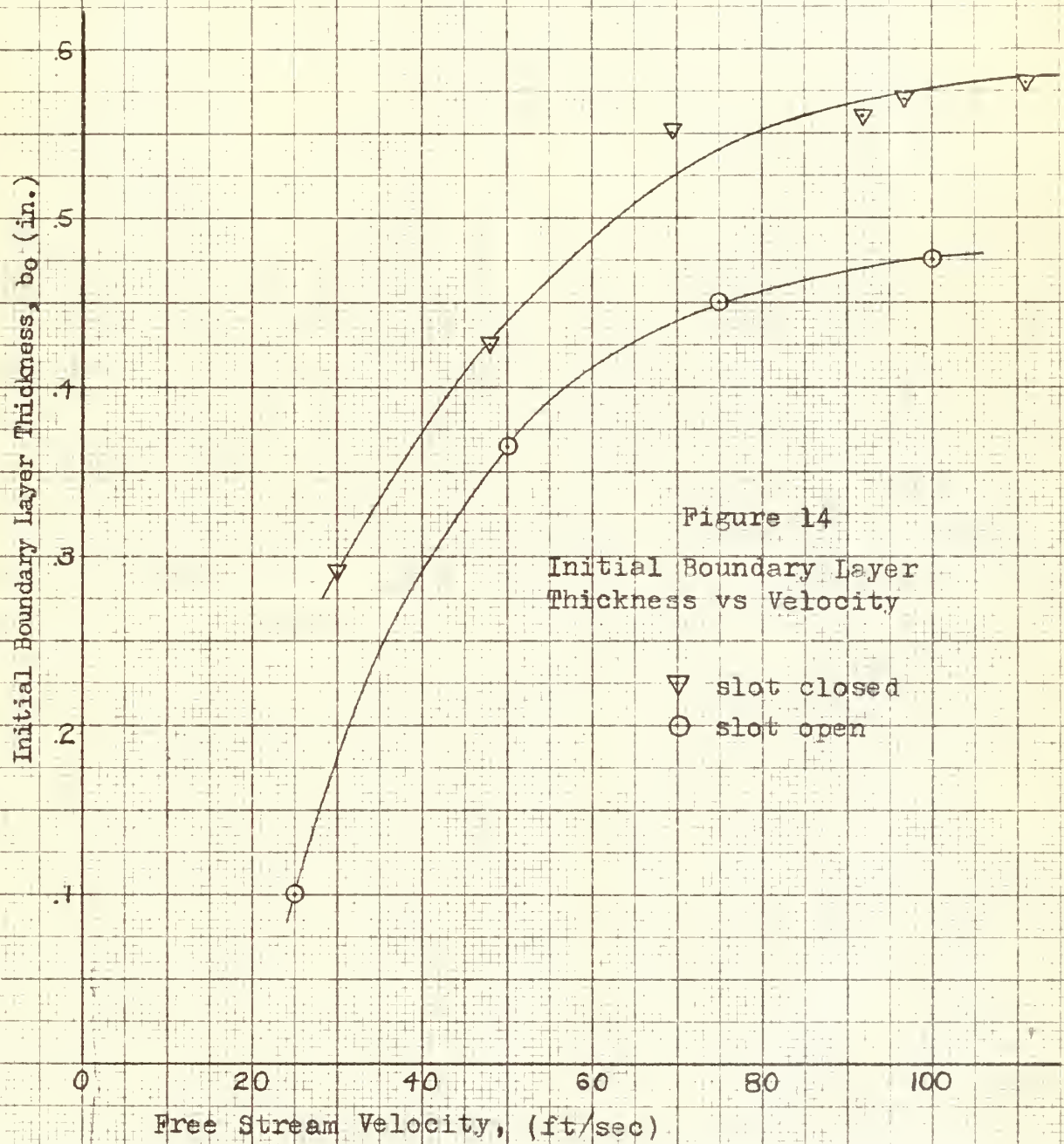
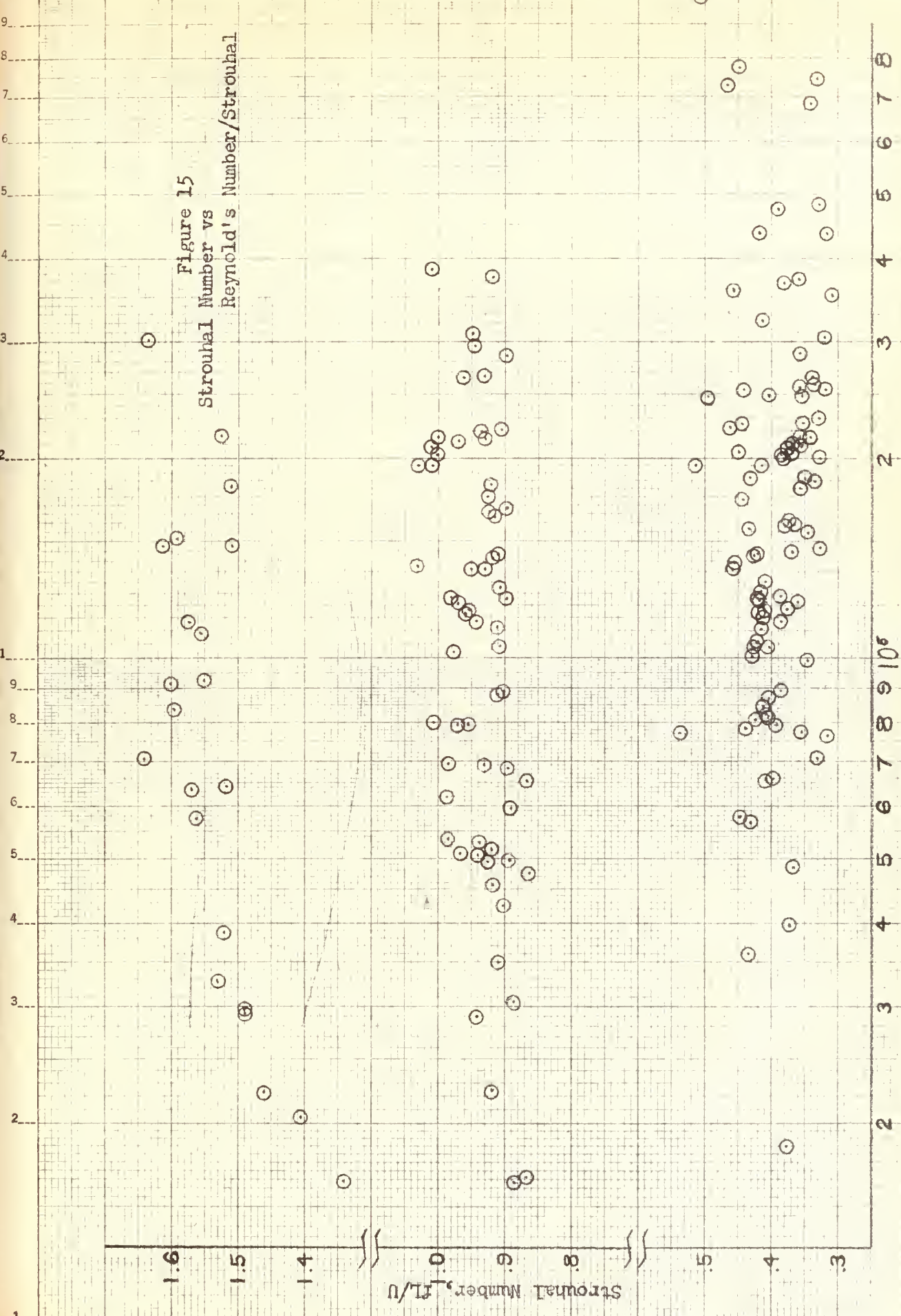


Figure 15

Strouhal Number vs
Reynold's Number/Strouhal



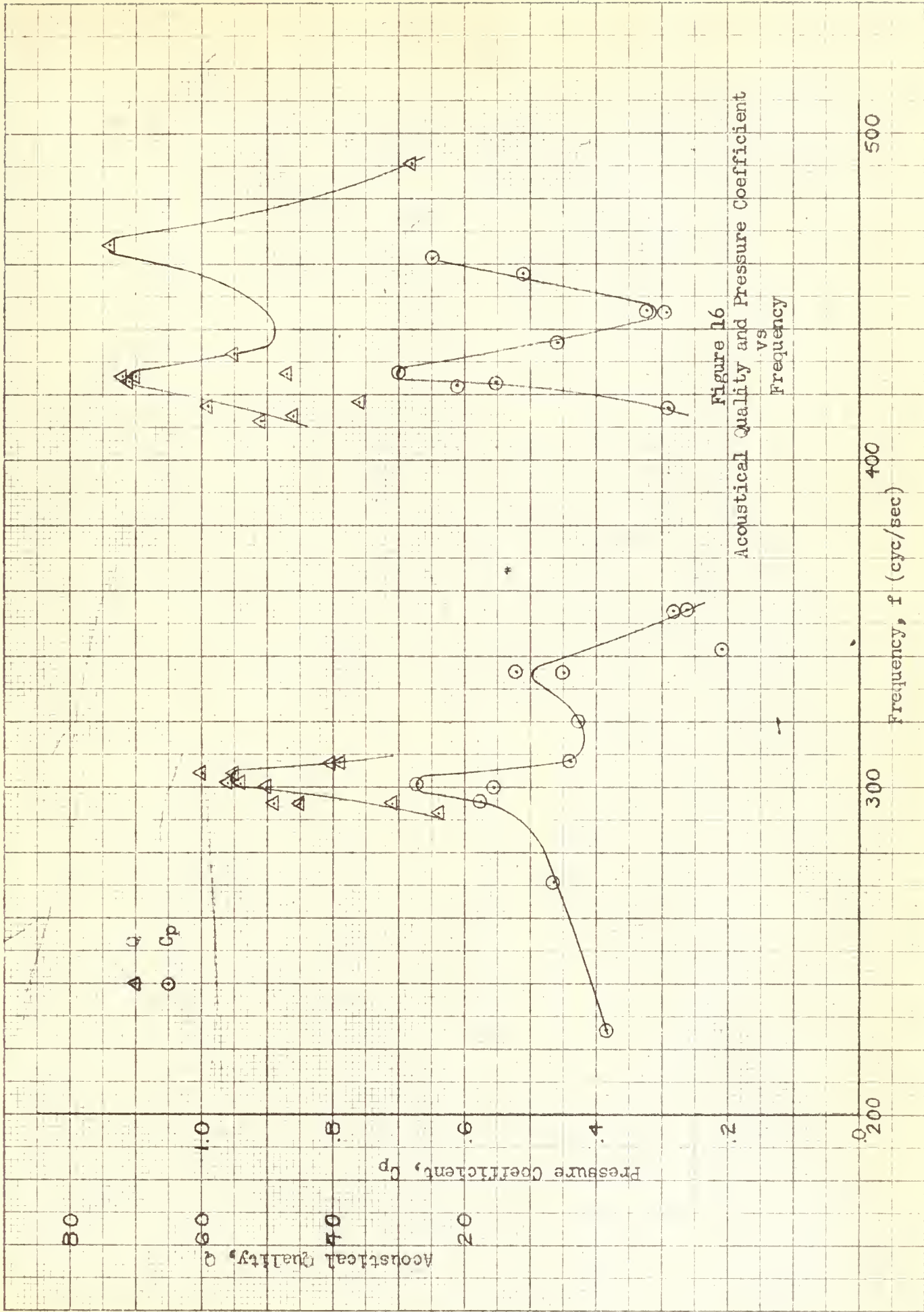
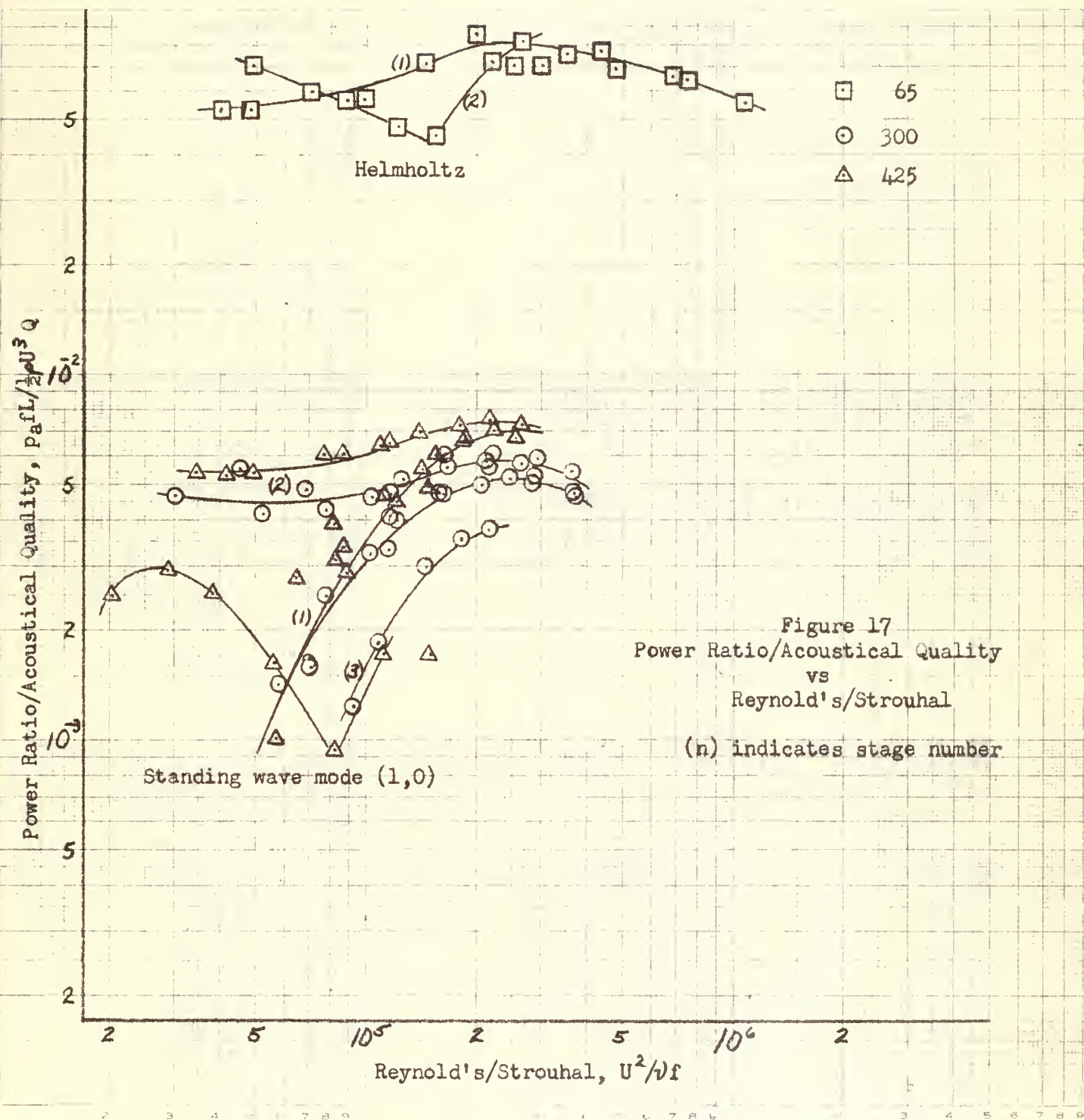


Figure 16
Acoustical Quality and Pressure Coefficient
vs
Frequency



APPENDIX III

A series of photographs

showing vortices in successive positions of travel across the slot.

$U = 31.0 \text{ ft/sec}$, $f = 31.6 \text{ cyc/sec}$, $L = 4.2 \text{ in.}$, $h = 47.5 \text{ in.}$







thesA99

Vortex formations caused by fluid flow a



3 2768 001 91090 4
DUDLEY KNOX LIBRARY